NASA Technical Paper 2890

1989

NASA SC(2)-0714 Airfoil Data Corrected for Sidewall Boundary-Layer Effects in the Langley 0.3-Meter Transonic Cryogenic Tunnel

Renaldo V. Jenkins
Langley Research Center
Hampton, Virginia

National Aeronautics and Space Administration
Office of Management
Scientific and Technical Information Division

Summary

This report presents aerodynamic data corrected for wall interference for the NASA SC(2)-0714 airfoil at Mach numbers from 0.60 to 0.76 and angles of attack from $-2.0°$ to $6.0°$. The test Reynolds numbers were 4×10^6 , 6×10^6, 10×10^6, 15×10^6, 30×10^6, 40×10^6, and 45×10^6 based on the 152.4-mm chord of the airfoil. Corrections for the effects of the tunnel sidewall boundary layer have been made. The uncorrected data were previously published in NASA Technical Memorandum 4044. The design goal of producing a 14-percent-thick transonic airfoil with a normal-force coefficient of 0.70 and a reasonable profile-drag coefficient at a Reynolds number of 40×10^6 was accomplished with the SC(2)-0714 airfoil. The airfoil has a drag-divergence Mach number of 0.726 and a profile-drag coefficient of 0.0098 at a corrected normal-force coefficient of 0.70.

Introduction

As part of the Advanced Technology Airfoil Tests (ATAT) program (see ref. 1), the NASA SC(2)-0714 airfoil was tested in the Langley 0.3-Meter Transonic Cryogenic Tunnel. The SC(2)-0714 transonic airfoil was designed to be 14 percent thick and have a normal-force coefficient of 0.70 at a Reynolds number of 40×10^6. The airfoil was tested at Mach numbers from 0.60 to 0.76 and an angle-of-attack range of $-2.0°$ to $6.0°$. The test Reynolds numbers were 4×10^6, 6×10^6, 10×10^6, 15×10^6, 30×10^6, 40×10^6, and 45×10^6 based on the 152.4-mm chord of the airfoil. The basic data, consisting of surface pressure distributions and integrated aerodynamic coefficients, are presented in reference 2. This report contains aerodynamic data which have been corrected for the effects of the tunnel sidewall boundary layer.

Symbols

b	airfoil model span, 203.2 mm
c	airfoil model chord, 152.4 mm
c_d	section profile-drag coefficient from wake measurement
c_m	section quarter-chord pitching-moment coefficient from model pressures
c_n	section normal-force coefficient from model pressures
C_p	pressure coefficient
M	free-stream Mach number
M_{dd}	drag-divergence Mach number (Mach number for which $dc_d/dM = 0.1$)
R	free-stream Reynolds number based on model chord
x	airfoil abscissa coordinate, mm
y	spanwise distance along model from centerline of tunnel and model (positive measured toward right-hand side), mm
z	airfoil ordinate coordinate, mm
α	angle of attack, deg
η	nondimensional spanwise distance based on tunnel half-span, $y/(b/2)$
Abbreviations:	
AOA	angle of attack
0.3-m TCT	0.3-Meter Transonic Cryogenic Tunnel
Airfoil designation:	
NASA SC(2)-0714	supercritical (phase 2), 0.7 design lift coefficient, 14 percent thick
Superscript:	
*	sonic condition (i.e., $M = 1.0$)

Subscript:

dd	at drag-divergence Mach number

Apparatus

Wind Tunnel

Tests of the SC(2)-0714 airfoil were conducted in the 8- by 24-in. two-dimensional test section of the Langley 0.3-m TCT. The 0.3-m TCT is a continuous-flow, fan-driven, transonic tunnel which uses nitrogen gas as the test medium. The tunnel is capable of operating at temperatures varying from about 78 K to about 327 K and stagnation pressures ranging from slightly greater than 1.0 atm up to 6.0 atm. Mach number can be varied from about 0.20 to 0.90. The ability to operate at cryogenic temperatures combined with the pressure capability of 6 atm provides a high Reynolds number capability at relatively low model loading. For this test, slotted walls were installed for the floor and ceiling to help reduce model blockage. Information on the design and operational capabilities of the 0.3-m TCT can be found in references 3 and 4. The use of cryogenic nitrogen as a test gas is discussed in reference 5. Discussions of the data acquisition system and data reduction technique for the 0.3-m TCT are given in references 6 and 7. Repeatability of the data is discussed in reference 8.

The two-dimensional test section contains computer driven angle-of-attack and momentum rake systems. The angle-of-attack system is capable of varying the angle of attack over a range of about 40°. The momentum rake (see fig. 1), located just downstream of the airfoil (see fig. 2), provides up to nine total-pressure measurements across the span of the model and can traverse vertically from about 1 chord above to about 1/2 chord below the model. Integration of these pressure measurements provides the wake drag force coefficient. The comparison of these spanwise pressure measurements provides a mechanism for determining the extent of the two-dimensionality in the flow.

Model

The SC(2)-0714 was designed at Langley Research Center. This airfoil is of the supercritical type and has a maximum thickness-to-chord ratio of 0.14 with a blunt trailing edge of 0.0077-chord thickness. This airfoil does not have the recess slot cut in the upper surface trailing edge as did the original airfoil (see ref. 9). The airfoil shape and pressure orifice layout are given in figure 3. The orifice layout is given as a planform of the model viewed from above while facing into the flow.

The model tested has a chord of 152.4 mm (6.0 in.) and was constructed of Armco PH 13-8 Mo stainless steel. The model was fabricated in two parts and these parts were bonded together with a structural adhesive film. The surface pressure tubing was placed inside the model by trenching the joining surfaces before the two parts were bonded. The static pressure orifices were made by drilling 0.254-mm holes normal to the model surface to meet the internal tubes. The model was designed to have 24 static pressure orifices on the upper surface and 24 orifices on the lower surface. However, only 22 orifices on the upper surface and 23 on the lower surface were suitable for use in the tests. In addition, there were 18 spanwise orifices on the upper surface.

The design and the measured coordinates for the model are given in table I, and the orifice locations are given in table II. The model contour was not within the desired tolerance of $0.0002c$ of the design values of the SC(2)-0714 coordinates. The upper surface was thinner than the design values. In fact, the first 2.0 percent was thinner by as much as $0.0013c$. The lower surface was generally thinner than the design values with excursions as great as $0.0015c$ within the first 2.0 percent of chord. The total contour of the model was smooth and continuous with a surface finish in the range from 0.102 to 0.2 μm (4 to 8 μin.).

Wake Rake

As previously mentioned, the airfoil drag force coefficient is determined using the wake rake shown in figure 1. For the present tests, the rake contained six active pitot tubes. Pitot tube 1 (the preferred measurement $\eta = 0$) was on the tunnel midspan. Pitot tube 2 was located 12.7 mm ($\eta = -0.125$) to the left of the tunnel midspan; tube 3 was 25.4 mm ($\eta = -0.250$) to the left of the tunnel midspan; tube 4 was 38.1 mm ($\eta = -0.375$) to the left of the tunnel midspan; tube 5 was 50.8 mm ($\eta = -0.500$) to the left of the tunnel midspan; and tube 6 was 76.2 mm ($\eta = -0.750$) to the left of the tunnel midspan. The tubes had an outside diameter of 1.52 mm (0.060 in.) and an inside diameter of 1.02 mm (0.040 in.). Nine static pressures were measured on the sidewall opposite the wake rake. The nine static pressure ports are arranged with one port midway between the tunnel

floor and ceiling and four each spaced 25.4 mm apart above and below this midpoint. Both the pitot and static pressure measurements were made in a plane located about 183 mm ($1.2c$) downstream of the model trailing edge.

Data Reduction

Section normal-force and quarter-chord pitching-moment coefficients are obtained through the numerical integrations of the surface pressure distributions. The local pressure measured at each orifice is multiplied by the incremental area over which that pressure acts to form the force distribution functions. The force distribution functions are integrated by the trapezoidal method. Section profile-drag coefficient is obtained from the rake pitot pressure measurements by computing the point drag coefficient by the method of reference 10 for each of the rake pitot tubes and rake position. These point drag coefficients are then numerically integrated over the wake by the trapezoidal method. The point drag coefficients are calculated under the assumption of zero pressure decrement outside the model wake, and they are corrected by applying the nonzero decrement correction during the integration. This correction is accomplished by comparing a "threshold" value to the individual point drag coefficients. If the point drag values are greater than or equal to the threshold, they are included in the integration; otherwise they are excluded. This correction is applied only for the extent of the wake over which the integration occurs. The area between threshold value and zero (which is bounded by the extent of the wake) is subtracted to give the section profile-drag coefficient c_d. The corrected section profile-drag coefficient c_d is thus corrected for both the extent of the wake and the nonzero pressure decrement outside the wake. For the present test, the threshold value was set at 0.0002 based on previous experience. The integration procedure checks the threshold value against the actual computed point drag values to assure that the assigned value is appropriate for each individual rake tube. If the assigned threshold value is not appropriate, the procedure chooses a computed point drag value that minimizes the error in the integration. Six section profile-drag coefficient values are presented in reference 2; however, only the centerline value is included in this report.

Uncorrected and Corrected Data

Uncorrected Data

Values of c_d, c_m, and α at constant normal-force coefficient and Reynolds number at various Mach numbers, obtained from large-scale plots of the data figures from reference 2, have been tabulated. A sample of these data is presented in the first four columns of table III. (The last four columns of this table contain data that have been corrected for sidewall boundary-layer effects and are discussed separately.) Plots of uncorrected profile-drag coefficient versus Mach number from these tabulations are presented for uncorrected normal-force coefficients in increments of 0.05 from 0.50 to 0.80 for each of the seven test Reynolds numbers in figure 4. Similarly, uncorrected pitching-moment coefficient values are plotted against Mach number in figure 5 for the same range of uncorrected normal-force coefficient values.

The drag-divergence Mach number is defined here as the Mach number for which $dc_d/dM = 0.1$. The drag-divergence Mach number M_{dd} and drag-divergence profile-drag coefficient $c_{d,dd}$ are obtained from the curves of figure 4. The drag-divergence pitching-moment coefficient $c_{m,dd}$ was obtained from curves like those of figure 5. Results of this procedure are tabulated in the first four columns of table IV.

Data Corrected for Wall Interference

The 0.3-m TCT is a slotted wind tunnel designed according to the classical linear wall interference precepts and empirical data of reference 11. The slotted top and bottom walls have nearly zero blockage (see ref. 11), and the corrections to the Mach number and flow curvature for their effect should be minimal. The solid sidewalls, on the other hand, have boundary layers which interact with the model pressure field and must be taken into account. A partial list of the available correction procedures is as follows:

1. Sidewalls only (refs. 12, 13, and 14)
2. Top and bottom walls only (refs. 15 and 16)
3. All four walls (refs. 17, 18, 19, and 20)

Experience with correcting two-dimensional data from this tunnel indicates (see refs. 8 and 21) that the data should be corrected for sidewall boundary-layer effects to get the change in Mach number and must be corrected for all four walls (see ref. 22) to get the change in both Mach number and angle of attack.

Figures 6 and 7, and 8 and 9, give two typical examples of the comparisons between theoretical calculations (made with the GRUMFOIL program, ref. 23) and both corrected and uncorrected data. In figure 6, the uncorrected data are compared with results obtained by specifying a measured Mach number of 0.736 and a normal-force coefficient of 0.4425 in the GRUMFOIL calculation. These low lift results show a slight disparity between the theory and experiment for both the upper and lower surfaces.

Using the tables of reference 14, the measured data were corrected for sidewalls only and compared with theoretical results in figure 7. (The tables of ref. 14 are based on the theory of refs. 12 and 13.) The corrected Mach number of 0.722 and a normal-force coefficient of 0.4483 were specified in GRUMFOIL. Figure 7 shows improved agreement between theory and experiment for both the upper and lower surfaces.

Uncorrected data for a high lift case are compared with theory in figure 8. The measured Mach number of 0.735 and normal-force coefficient of 0.8598 were specified for the calculation. These results show disagreement between theory and experiment, particularly at the shock location on the upper surface. Correcting these data by the tables yields a Mach number of 0.721 and a normal-force coefficient of 0.8710. The comparison between theory and experiment is shown in figure 9. The agreement is much improved, particularly at the shock location.

The sidewall-only correction significantly improves the agreement between theory and experiment and is relatively ease to apply. In view of this agreement and the results of reference 8, it was decided that the sidewall-only correction would be used in this report.

The data from the first three columns of table III were corrected using reference 14 (sidewalls only) to produce columns 5, 6, and 7. Column 8 of table III is the corrected normal-force coefficient. Applying sidewall-only correction to the first four columns of the drag-divergence data in table IV gives the corrected data in the last four columns.

Presentation of Data

Data are presented in tables as follows:

Table	Reynolds number, R	Type of data	Page
III	40×10^6	Cross-plotted	9
IV	4×10^6 to 45×10^6	Drag divergence	10
V	4×10^6 to 40×10^6	Reynolds number effects at design c_n	13

The remaining data are presented in figures as follows:

Results and Discussion

Table IV, which contains a summary of the drag-divergence conditions for the airfoil, can be used to estimate the optimal cruise parameters at any normal-force coefficient and Reynolds number in the test envelope. This table was used to obtain the drag-divergence conditions at the airfoil design normal-force coefficient of 0.70 and Reynolds number of 40×10^6. Two sets of conditions meet the drag-divergence definition at an uncorrected normal-force coefficient of 0.70. The higher uncorrected drag-divergence Mach number of 0.740 was chosen. (The broken lines in subsequent figures (see fig. 15 for example) are for the lower Mach number conditions.) The corresponding uncorrected drag-divergence profile-drag coefficient is 0.0097. Interpolating in the tables to a corrected normal-force coefficient of 0.70 gives the corrected drag-divergence Mach number as 0.726, profile-drag coefficient as 0.0098, and quarter-chord pitching moment as -0.1783. (These are respectable values for

10. Baals, Donald D.; and Mourhess, Mary J.: *Numerical Evaluation of the Wake-Survey Equations for Subsonic Flow Including the Effect of Energy Addition.* NACA WR L-5, 1945. (Formerly NACA ARR L5H27.)
11. Barnwell, Richard W.: *Design and Performance Evaluation of Slotted Walls for Two-Dimensional Wind Tunnels.* NASA TM-78648, 1978.
12. Barnwell, Richard W.: Similarity Rule for Sidewall Boundary-Layer Effect in Two-Dimensional Wind Tunnels. *AIAA J.*, vol. 18, no. 9, Sept. 1980, pp. 1149–1151.
13. Sewall, William G.: The Effects of Sidewall Boundary Layers in Two-Dimensional Subsonic and Transonic Wind Tunnels. *AIAA J.*, vol. 20, no. 9, Sept. 1982, pp. 1253–1256.
14. Jenkins, Renaldo V.; and Adcock, Jerry B.: *Tables for Correcting Airfoil Data Obtained in the Langley 0.3-Meter Transonic Cryogenic Tunnel for Sidewall Boundary Layer Effects.* NASA TM-87723, 1986.
15. Murman, E. M.: A Correction Method for Transonic Wind Tunnel Wall Interference. AIAA-79-1533, July 1979.
16. Kemp, William B., Jr.: *TWINTAN: A Program for Transonic Wall Interference Assessment in Two-Dimensional Wind Tunnels.* NASA TM-81819, 1980.
17. Kemp, William B., Jr.; and Adcock, Jerry B.: Combined Four-Wall Interference Assessment in Two-Dimensional Airfoil Tests. AIAA-82-0586, Mar. 1982.
18. Kemp, William B., Jr.: *TWINTN4: A Program for Transonic Four-Wall Interference Assessment in Two-Dimensional Wind Tunnels.* NASA CR-3777, 1984.
19. Gumbert, Clyde R.; and Newman, Perry A.: Validation of a Wall-Interference Assessment/Correction Procedure for Airfoil Tests in the Langley 0.3-Meter Transonic Cryogenic Tunnel. AIAA-84-2151, Aug. 1984.
20. Murthy, A. V.: *A Simplified Fourwall Interference Assessment Procedure for Airfoil Data Obtained in the Langley 0.3-Meter Transonic Cryogenic Tunnel.* NASA CR-4042, 1987.
21. Jenkins, Renaldo V.: Some Experience With Barnwell-Sewall Type Correction to Two-Dimensional Airfoil Data. *Wind Tunnel Wall Interference Assessment/Correction—1983*, Perry A. Newman and Richard W. Barnwell, eds., NASA CP-2319, 1984, pp. 375–392.
22. Gumbert, Clyde R.; Newman, Perry A.; Kemp, William B., Jr.; and Adcock, Jerry B.: Adaptation of a Four-Wall Interference Assessment/Correction Procedure for Airfoil Tests in the 0.3-m TCT. *Wind Tunnel Wall Interference Assessment/Correction—1983*, Perry A. Newman and Richard W. Barnwell, eds., NASA CP-2319, 1984, pp. 393–411.
23. Melnik, R. E.: Turbulent Interactions on Airfoils at Transonic Speeds—Recent Developments. *Computation of Viscous-Inviscid Interactions*, AGARD-CP-291, Feb. 1981, pp. 10-1–10-34.

Table I. Coordinates for the NASA SC(2)-0714 Airfoil

Upper surface			
	z/c		
x/c	Design	Measured	Change
0.0000	0.0000	0.0000	0.0000
.0020	.0108	.0095	−.0013
.0050	.0167	.0158	−.0009
.0100	.0225	.0219	−.0006
.0200	.0297	.0293	−.0004
.0300	.0346	.0343	−.0003
.0400	.0383	.0381	−.0002
.0500	.0414	.0411	−.0003
.0700	.0463	.0462	−.0001
.1000	.0519	.0518	−.0001
.1200	.0549	.0548	−.0001
.1500	.0585	.0585	.0000
.1700	.0606	.0606	.0000
.2000	.0632	.0632	.0000
.2200	.0647	.0646	−.0001
.2500	.0665	.0664	−.0001
.2700	.0675	.0673	−.0002
.3000	.0686	.0685	−.0001
.3300	.0694	.0692	−.0002
.3500	.0698	.0696	−.0002
.3800	.0700	.0698	−.0002
.4000	.0700	.0697	−.0003
.4300	.0697	.0695	−.0002
.4500	.0694	.0692	−.0002
.4800	.0686	.0684	−.0002
.5000	.0680	.0678	−.0002
.5300	.0668	.0666	−.0002
.5500	.0658	.0656	−.0002
.5700	.0646	.0645	−.0001
.6000	.0627	.0625	−.0002
.6200	.0613	.0610	−.0002
.6500	.0587	.0585	−.0002
.6800	.0558	.0555	−.0003
.7000	.0536	.0533	−.0003
.7200	.0512	.0509	−.0003
.7500	.0472	.0469	−.0003
.7700	.0442	.0439	−.0003
.8000	.0392	.0389	−.0003
.8200	.0356	.0353	−.0003
.8500	.0297	.0294	−.0003
.8700	.0255	.0251	−.0004
.9000	.0186	.0181	−.0005
.9200	.0137	.0131	−.0006
.9500	.0057	.0049	−.0008
.9700	.0000	−.0009	−.0009
.9800	−.0030	−.0039	−.0009
.9900	−.0062	−.0071	−.0009
1.0000	[a]− .0088	−.0104	−.0016

Lower surface			
	z/c		
x/c	Design	Measured	Change
0.0000	0.0000	0.0000	0.0000
.0020	−.0108	−.0093	.0015
.0050	−.0165	−.0160	.0005
.0100	−.0223	−.0221	.0002
.0200	−.0295	−.0295	.0000
.0300	−.0343	−.0344	−.0001
.0400	−.0381	−.0381	.0000
.0500	−.0411	−.0412	−.0001
.0700	−.0461	−.0462	−.0001
.1000	−.0517	−.0517	.0000
.1200	−.0547	−.0547	.0000
.1500	−.0585	−.0585	.0000
.1700	−.0606	−.0606	.0000
.2000	−.0633	−.0633	.0000
.2200	−.0648	−.0647	.0001
.2500	−.0667	−.0666	.0001
.2800	−.0681	−.0680	.0001
.3000	−.0688	−.0687	.0001
.3200	−.0693	−.0692	.0001
.3500	−.0697	−.0696	.0001
.3700	−.0697	−.0696	.0001
.4000	−.0693	−.0692	.0001
.4200	−.0689	−.0688	.0001
.4500	−.0678	−.0676	.0001
.4800	−.0661	−.0657	.0004
.5000	−.0646	−.0644	.0002
.5300	−.0616	−.0614	.0002
.5500	−.0591	−.0588	.0003
.5800	−.0546	−.0643	.0003
.6000	−.0511	−.0509	.0002
.6300	−.0454	−.0451	.0003
.6500	−.0413	−.0410	.0003
.6800	−.0349	−.0346	.0003
.7000	−.0305	−.0302	.0003
.7300	−.0239	−.0235	.0004
.7500	−.0195	−.0192	.0003
.7700	−.0152	−.0150	.0002
.8000	−.0095	−.0093	.0002
.8300	−.0050	−.0048	.0002
.8500	−.0028	−.0027	.0001
.8700	−.0014	−.0013	.0001
.8900	−.0008	−.0008	.0000
.9200	−.0016	−.0016	.0000
.9400	−.0034	−.0035	−.0001
.9500	−.0049	−.0049	.0000
.9600	−.0066	−.0066	.0000
.9700	−.0086	−.0085	.0001
.9800	−.0109	−.0109	.0000
.9900	−.0136	−.0137	−.0001
1.0000	−.0165	−.0163	.0001

[a]The original airfoil did not have a blunt trailing edge, and thus this value was not defined.

Table II. Orifice Locations

(a) Chordwise orifices

Upper surface		
x/c	z/c	y/c
0.0000	0.0000	0.0000
.0132	.0247	.0437
.0254	.0322	.0683
.0501	.0411	.0218
[a].0752	.0472	.0217
.1006	.0518	.0223
.1503	.0584	.0229
.2002	.0632	.0231
.2503	.0664	.0215
.3000	.0685	.0217
.3501	.0696	.0219
.4001	.0697	.0215
.4500	.0691	.0214
.5001	.0678	.0218
.5501	.0656	.0212
.6002	.0625	.0210
.6502	.0584	.0215
.7004	.0533	.0214
.7500	.0469	.0211
.8000	.0389	.0213
[a].8504	.0294	.0216
.9001	.0181	.0218
.9502	.0049	.0649
1.0000	−.0128	.0000

Lower surface		
x/c	z/c	y/c
0.0000	0.0000	0.0000
.0134	−.0252	−.0590
.0255	−.0325	−.0830
.0513	−.0416	−.0354
.0750	−.0473	−.0223
.1005	−.0519	−.0216
.1503	−.0586	−.0216
.2002	−.0633	−.0218
.2505	−.0667	−.0217
.3004	−.0688	−.0219
.3500	−.0697	−.0217
.4003	−.0692	−.0217
.4502	−.0677	−.0217
.5003	−.0644	−.0216
.5502	−.0589	−.0217
.6001	−.0510	−.0217
.6500	−.0410	−.0216
.7002	−.0302	−.0217
.7497	−.0192	−.0216
.8000	−.0093	−.0216
[a].8502	−.0027	−.0215
.9004	−.0007	−.0218
.9476	−.0046	−.0408
1.0000	−.0128	.0000

[a]This orifice either leaked or was blocked, and data from it were not included in the integrations to obtain the aerodynamic coefficients.

(b) Upper-surface spanwise orifices

$x/c = 0.1503$ $z/c = 0.0585$	$x/c = 0.5001$ $z/c = 0.0678$	$x/c = 0.8002$ $z/c = 0.0390$
y/c	y/c	y/c
0.5017	−0.5020	−0.5019
−.3347	−.3350	−.3352
−.1680	−.1691	−.1686
.1652	.1645	.1649
.3323	.3313	.3316
.4993	.4980	.4983

Table III. Cross-Plotted Data at a Reynolds Number of 40×10^6

$[c_n = 0.70]$

Uncorrected data			
M	c_d	c_m	α, deg
0.601	0.00820	−0.1600	1.36
.651	.00857	−.1653	1.23
.701	.00902	−.1690	.96
.711	.00899	−.1718	.86
.721	.00905	−.1738	.77
.731	.00922	−.1755	.72
.735	.00970	−.1770	.68
.740	.00977	−.1795	.59
.751	.01206	−.1910	.50
.760	.01433	−.1967	.48

Data corrected by tables of reference 14			
M	c_d	c_m	c_n
0.588	0.00832	−0.1624	0.7105
.637	.00869	−.1666	.7098
.687	.00915	−.1714	.7098
.697	.00912	−.1742	.7098
.707	.00917	−.1762	.7091
.717	.00934	−.1778	.7091
.721	.00983	−.1793	.7091
.726	.00990	−.1818	.7091
.737	.01222	−.1935	.7091
.746	.01453	−.1993	.7091

Table IV. Conditions at Drag Divergence

(a) $R = 4 \times 10^6$

Uncorrected data			
c_n	$c_{d,dd}$	M_{dd}	$c_{m,dd}$
0.70	0.01012	0.741	−0.1783
.75	.01046	.741	−.1793
.80	.01117	.741	−.1818
.85	.01230	.721	−.1888
1.00	.01738	.720	−.1845

Data corrected by tables of reference 14			
c_n	$c_{d,dd}$	M_{dd}	$c_{m,dd}$
0.71	0.01030	0.721	−0.1815
.76	.01065	.721	−.1825
.81	.01137	.721	−.1851
.86	.01252	.721	−.1922
1.02	.01771	.700	−.1880

(b) $R = 6 \times 10^6$

Uncorrected data			
c_n	$c_{d,dd}$	M_{dd}	$c_{m,dd}$
0.70	0.01212	0.741	−0.1625
.75	.01266	.741	−.1648
.80	.01353	.741	−.1705
.85	.01409	.731	−.1685
.90	.01560	.731	−.1740
.95	.01870	.731	−.1819

Data corrected by tables of reference 14			
c_n	$c_{d,dd}$	M_{dd}	$c_{m,dd}$
0.71	0.01233	0.722	−0.1653
.76	.01288	.722	−.1676
.81	.01376	.722	−.1734
.86	.01433	.712	−.1714
.92	.01587	.712	−.1770
.97	.01902	.707	−.1850

(c) $R = 10 \times 10^6$

Uncorrected data			
c_n	$c_{d,dd}$	M_{dd}	$c_{m,dd}$
0.60	0.01184	0.753	−0.1625
.65	.01216	.753	−.1650
.70	.01277	.753	−.1680
.75	.01179	.730	−.1605
.80	.01250	.730	−.1625
.85	.01379	.730	−.1650
.90	.01506	.730	−.1690
.95	.01784	.730	−.1750

Data corrected by tables of reference 14			
c_n	$c_{d,dd}$	M_{dd}	$c_{m,dd}$
0.61	0.01203	0.736	−0.1651
.66	.01235	.736	−.1676
.71	.01297	.736	−.1707
.76	.01198	.713	−.1631
.81	.01270	.713	−.1651
.86	.01401	.713	−.1676
.91	.01530	.713	−.1717
.97	.01813	.713	−.1778

Table IV. Continued

(d) $R = 15 \times 10^6$

Uncorrected data			
c_n	$c_{d,dd}$	M_{dd}	$c_{m,dd}$
0.60	0.01060	0.741	−0.1660
.65	.01080	.741	−.1673
.70	.01116	.741	−.1683
.75	.01176	.741	−.1700
.80	.01169	.730	−.1665
.85	.01280	.730	−.1687
.90	.01436	.730	−.1715
.95	.01692	.730	−.1787
1.00	.01960	.721	−.1783
1.05	.02480	.721	−.1838

Data corrected by tables of reference 14			
c_n	$c_{d,dd}$	M_{dd}	$c_{m,dd}$
0.61	0.01076	0.725	−0.1685
.66	.01096	.725	−.1698
.71	.01133	.725	−.1708
.76	.01194	.725	−.1726
.81	.01187	.714	−.1690
.86	.01297	.714	−.1712
.91	.01458	.714	−.1741
.96	.01717	.714	−.1814
1.02	.01989	.705	−.1810
1.07	.02517	.705	−.1866

(e) $R = 30 \times 10^6$

Uncorrected data			
c_n	$c_{d,dd}$	M_{dd}	$c_{m,dd}$
0.65	0.01000	0.742	−0.1786
.70	.01053	.742	−.1786
.75	.01017	.731	−.1737
.80	.01113	.731	−.1755
.85	.01052	.701	−.1656
.85	.01132	.721	−.1741
.90	.01275	.721	−.1765
.95	.01490	.721	−.1808
1.00	.01760	.721	−.1850
1.05	.02200	.721	−.1890

Data corrected by tables of reference 14			
c_n	$c_{d,dd}$	M_{dd}	$c_{m,dd}$
0.66	0.01014	0.727	−0.1811
.71	.01068	.727	−.1811
.76	.01031	.716	−.1761
.81	.01129	.716	−.1780
.86	.01067	.686	−.1678
.86	.01148	.706	−.1765
.91	.01293	.706	−.1790
.96	.01511	.706	−.1833
1.01	.01785	.706	−.1876
1.06	.02231	.706	−.1917

Table IV. Concluded

(f) $R = 40 \times 10^6$

Uncorrected data			
c_n	$c_{d,dd}$	M_{dd}	$c_{m,dd}$
0.55	0.00958	0.751	−0.1818
.60	.00917	.740	−.1773
.65	.00927	.740	−.1780
.70	.00922	.731	−.1755
.70	.00977	.740	−.1795
.75	.00957	.731	−.1765
.80	.00958	.721	−.1730
.85	.01036	.721	−.1738
.90	.01186	.721	−.1763
.95	.01414	.721	−.1805
1.00	.01724	.721	−.1855
1.05	.02130	.721	−.1935
1.10	.02500	.711	−.1900

Data corrected by tables of reference 14			
c_n	$c_{d,dd}$	M_{dd}	$c_{m,dd}$
0.56	0.00970	0.737	−0.1842
.61	.00929	.726	−.1796
.66	.00939	.726	−.1803
.71	.00990	.726	−.1818
.71	.00934	.717	−.1778
.76	.00969	.717	−.1788
.81	.00970	.707	−.1752
.86	.01049	.707	−.1761
.91	.01201	.707	−.1786
.96	.01432	.707	−.1828
1.01	.01746	.707	−.1879
1.06	.02158	.707	−.1960
1.11	.02535	.697	−.1927

(g) $R = 45 \times 10^6$

Uncorrected data			
c_n	$c_{d,dd}$	M_{dd}	$c_{m,dd}$
0.75	0.00947	0.731	−0.1780
.80	.00960	.720	−.1740
.85	.01026	.720	−.1750

Data corrected by tables of reference 14			
c_n	$c_{d,dd}$	M_{dd}	$c_{m,dd}$
0.76	0.00959	0.717	−0.1803
.81	.00972	.706	−.1763
.86	.01039	.706	−.1773

Table V. Effects of Reynolds Number on Drag-Divergence Conditions at the Design Normal-Force Coefficient

$[c_n = 0.70]$

Uncorrected data			
R	$c_{d,dd}$	M_{dd}	$c_{m,dd}$
4×10^6	0.01012	0.741	−0.1783
6×10^6	.01212	.741	−.1625
10×10^6	.01277	.753	−.1680
15×10^6	.01116	.741	−.1683
30×10^6	.01053	.742	−.1786
40×10^6	.00977	.740	−.1795

Data corrected by tables of reference 14			
c_n	$c_{d,dd}$	M_{dd}	$c_{m,dd}$
0.7126	0.01030	0.721	−0.1815
.7119	.01233	.722	−.1653
.7112	.01297	.736	−.1707
.7105	.01133	.725	−.1708
.7098	.01068	.727	−.1811
.7091	.00990	.726	−.1818

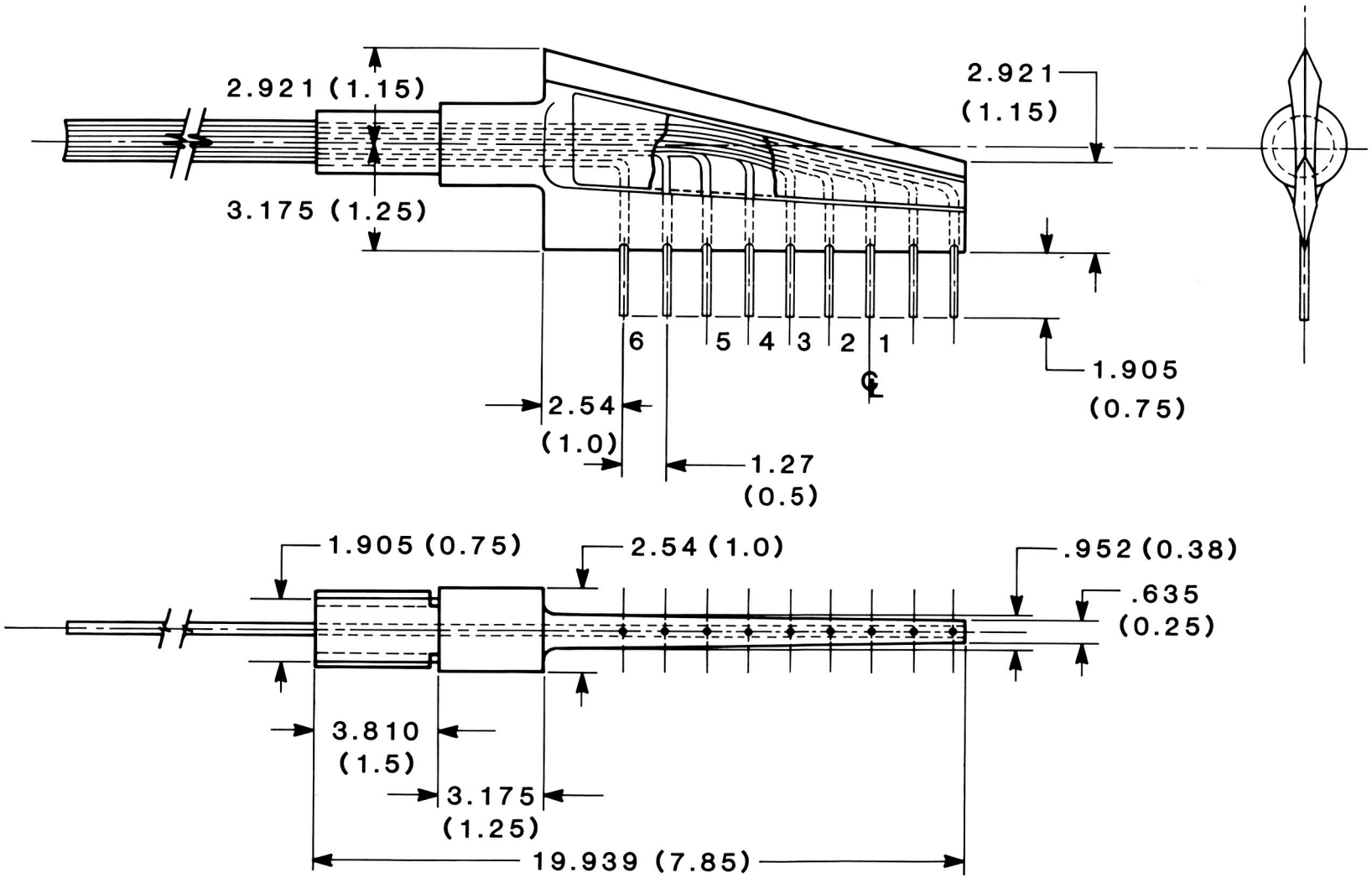

Figure 1. Details of wake survey (momentum) probe. All linear dimensions in centimeters (inches).

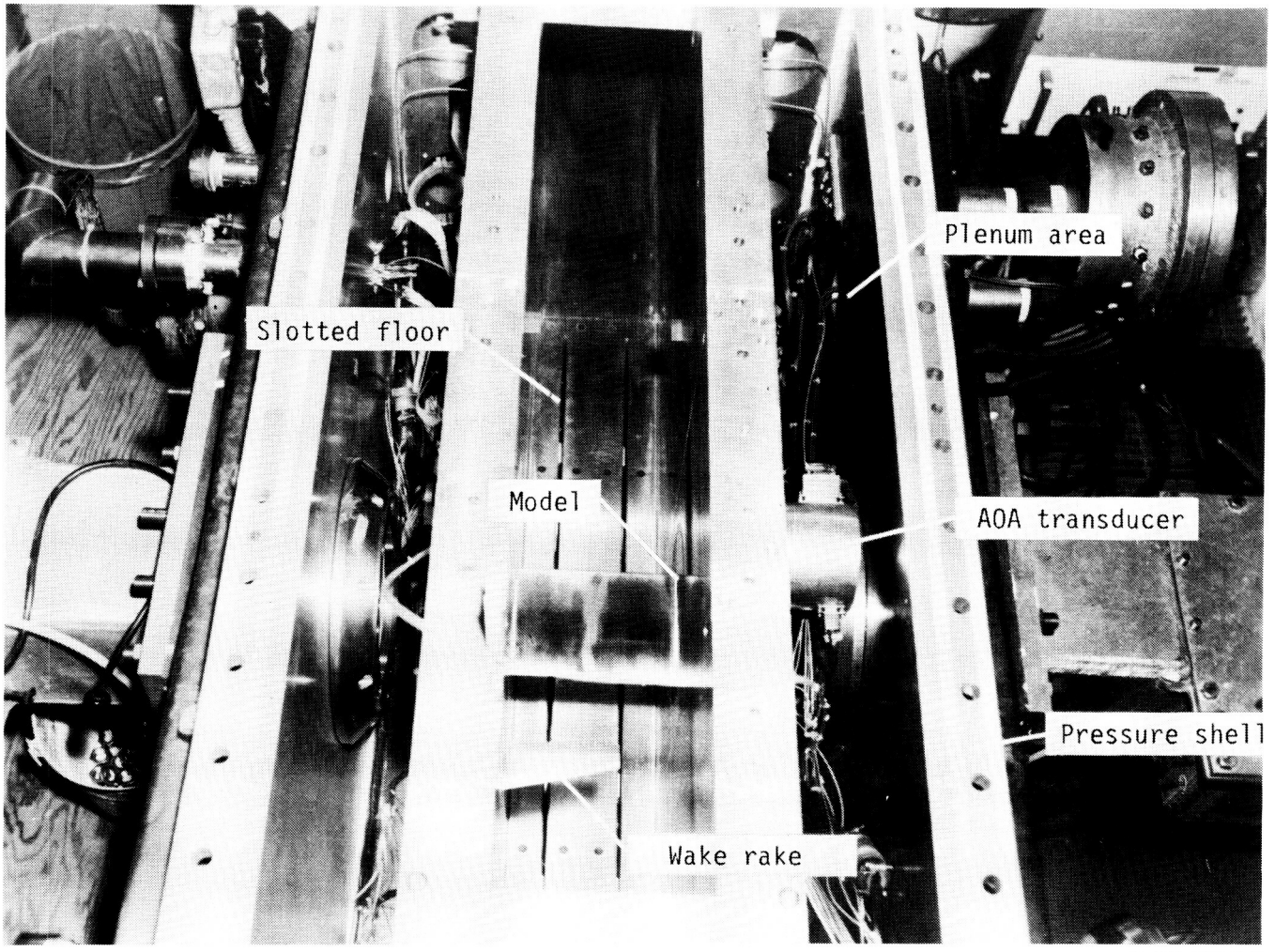

L-79-8913.2

Figure 2. Top-view photograph of two-dimensional test section of 0.3-m TCT.

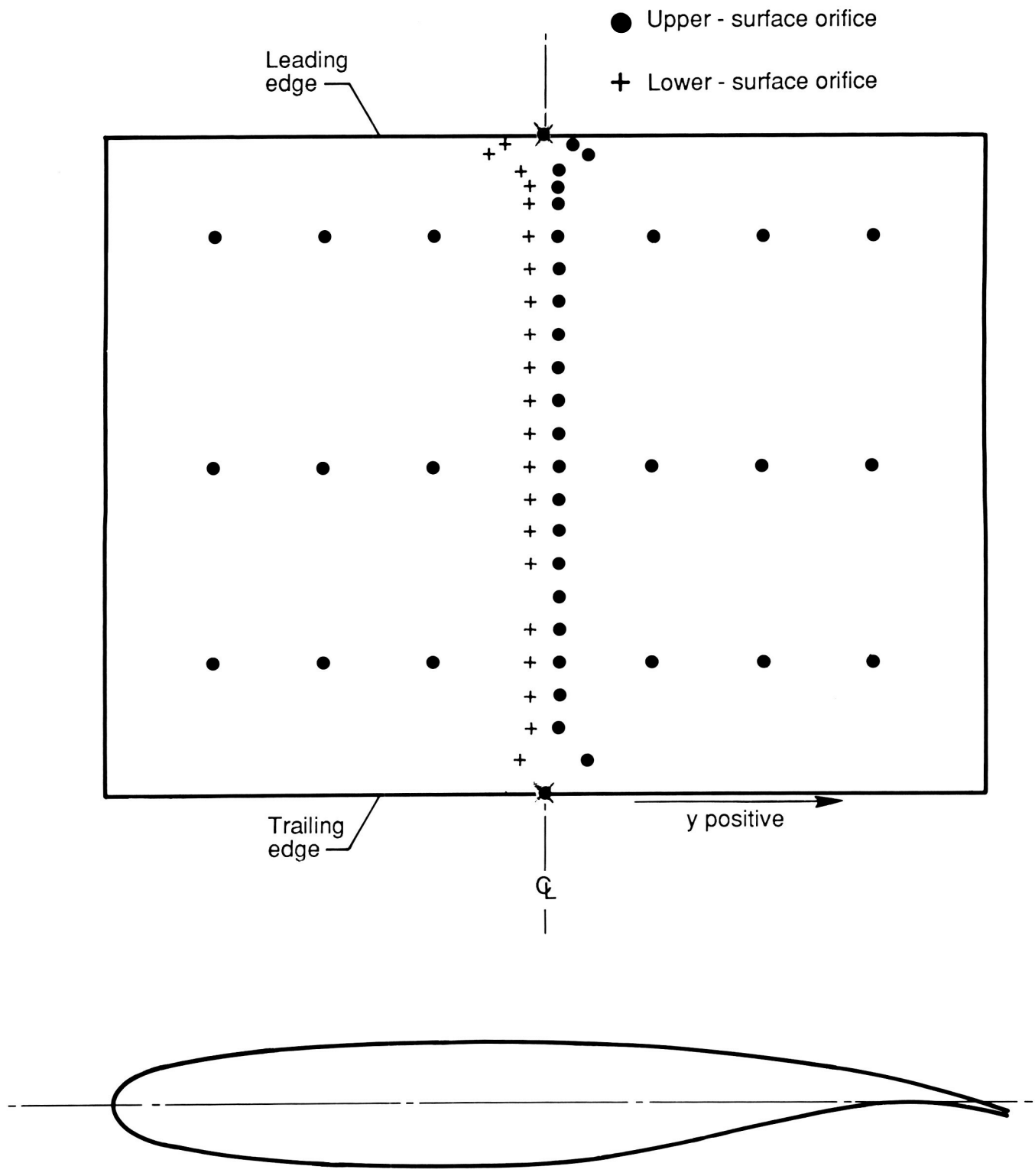

Figure 3. The NASA SC(2)-0714 airfoil shape and layout of its surface pressure orifices.

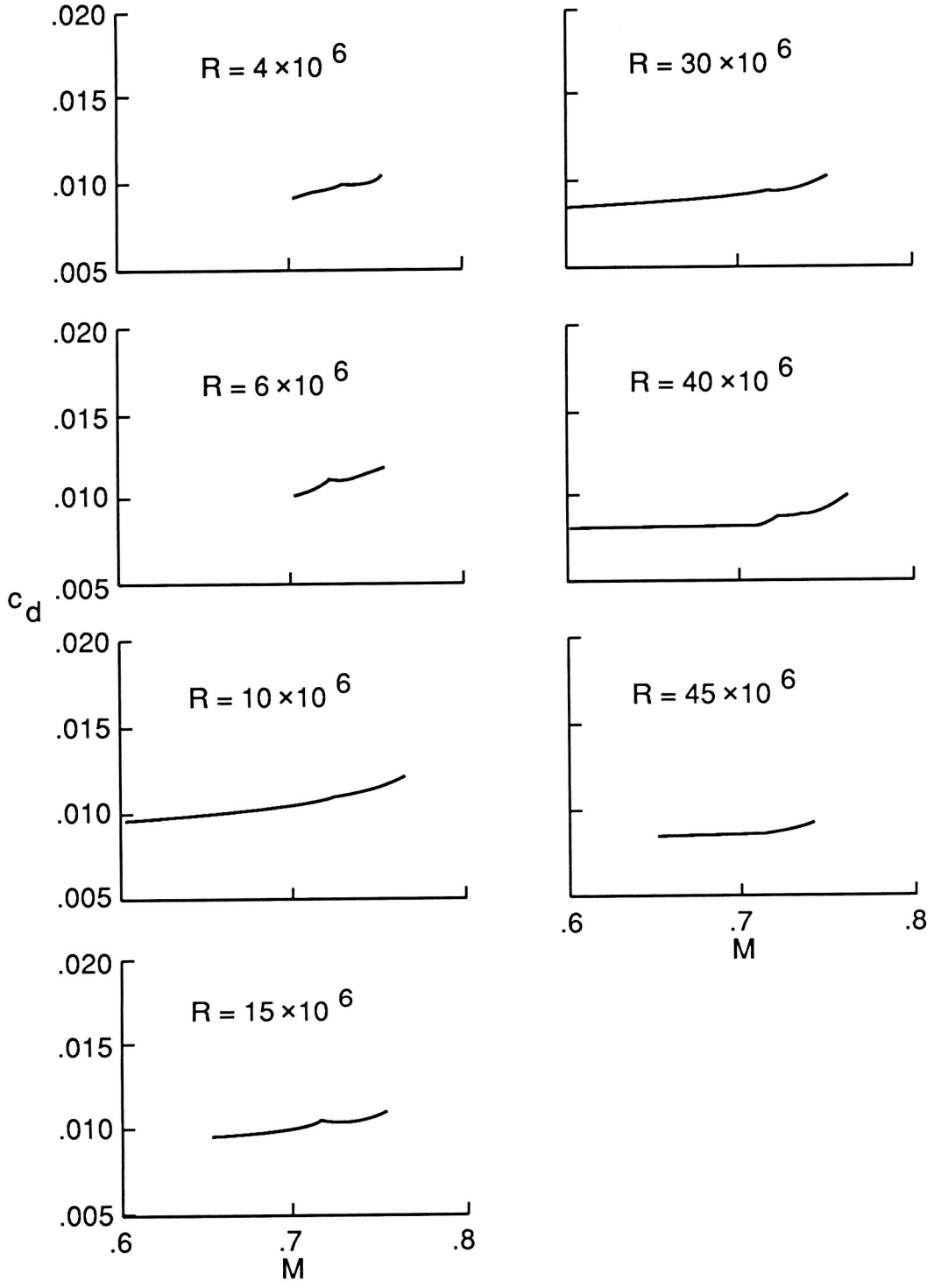

(a) $c_n = 0.50$.

Figure 4. Cross plots of profile-drag coefficient versus Mach number at various normal-force coefficients. Uncorrected data.

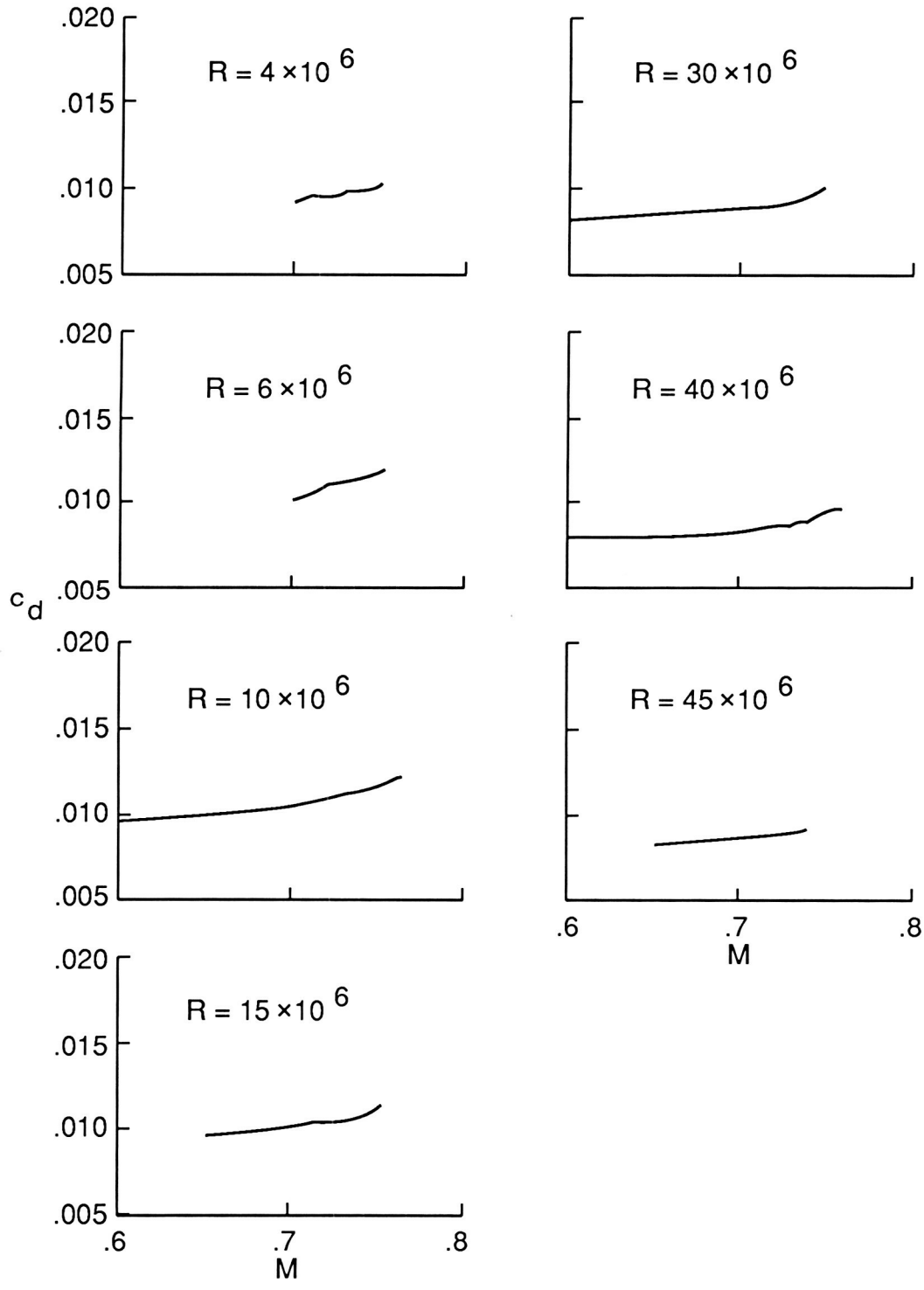

(b) $c_n = 0.55$.

Figure 4. Continued.

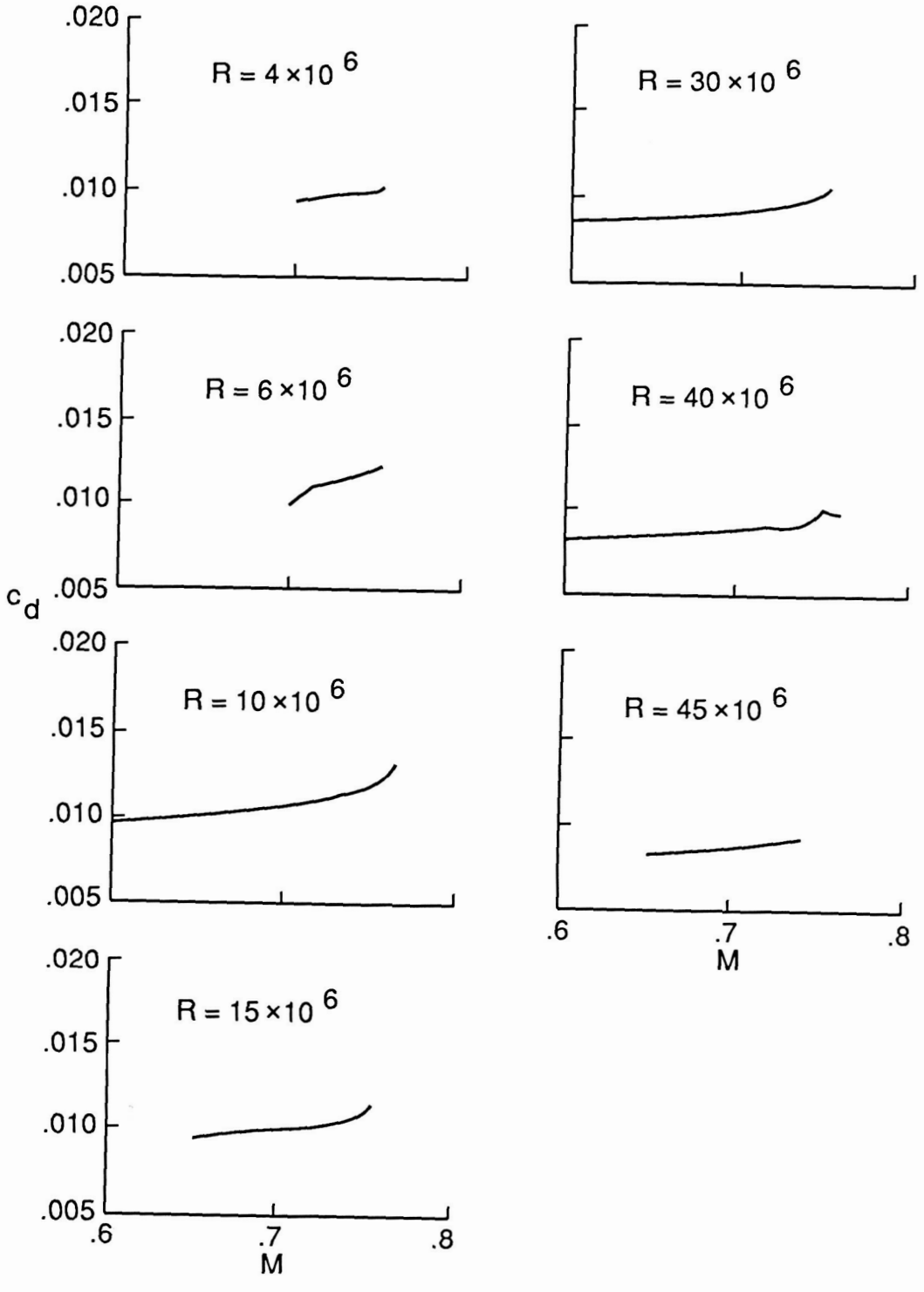

(c) $c_n = 0.60$.

Figure 4. Continued.

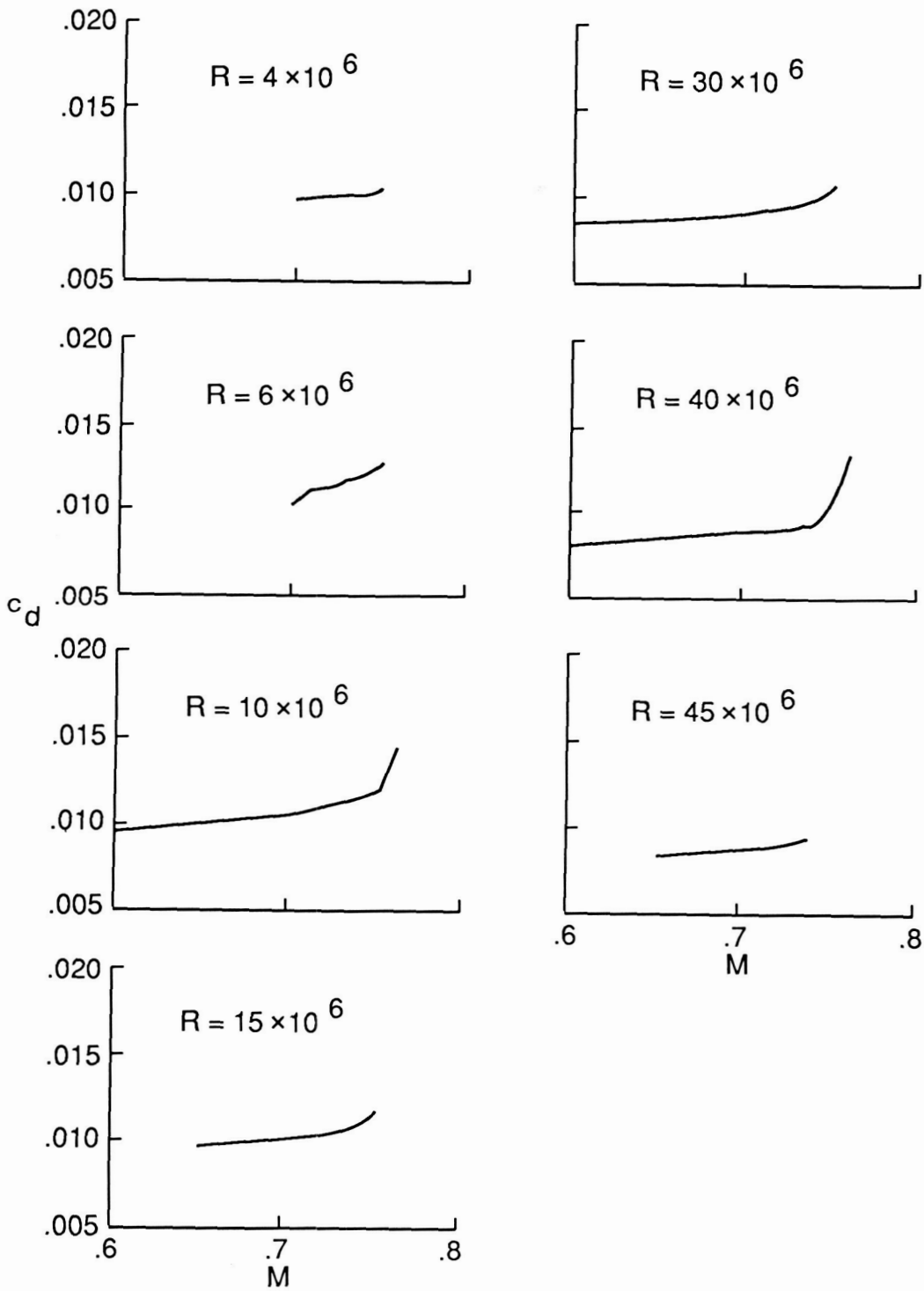

(d) $c_n = 0.65$.

Figure 4. Continued.

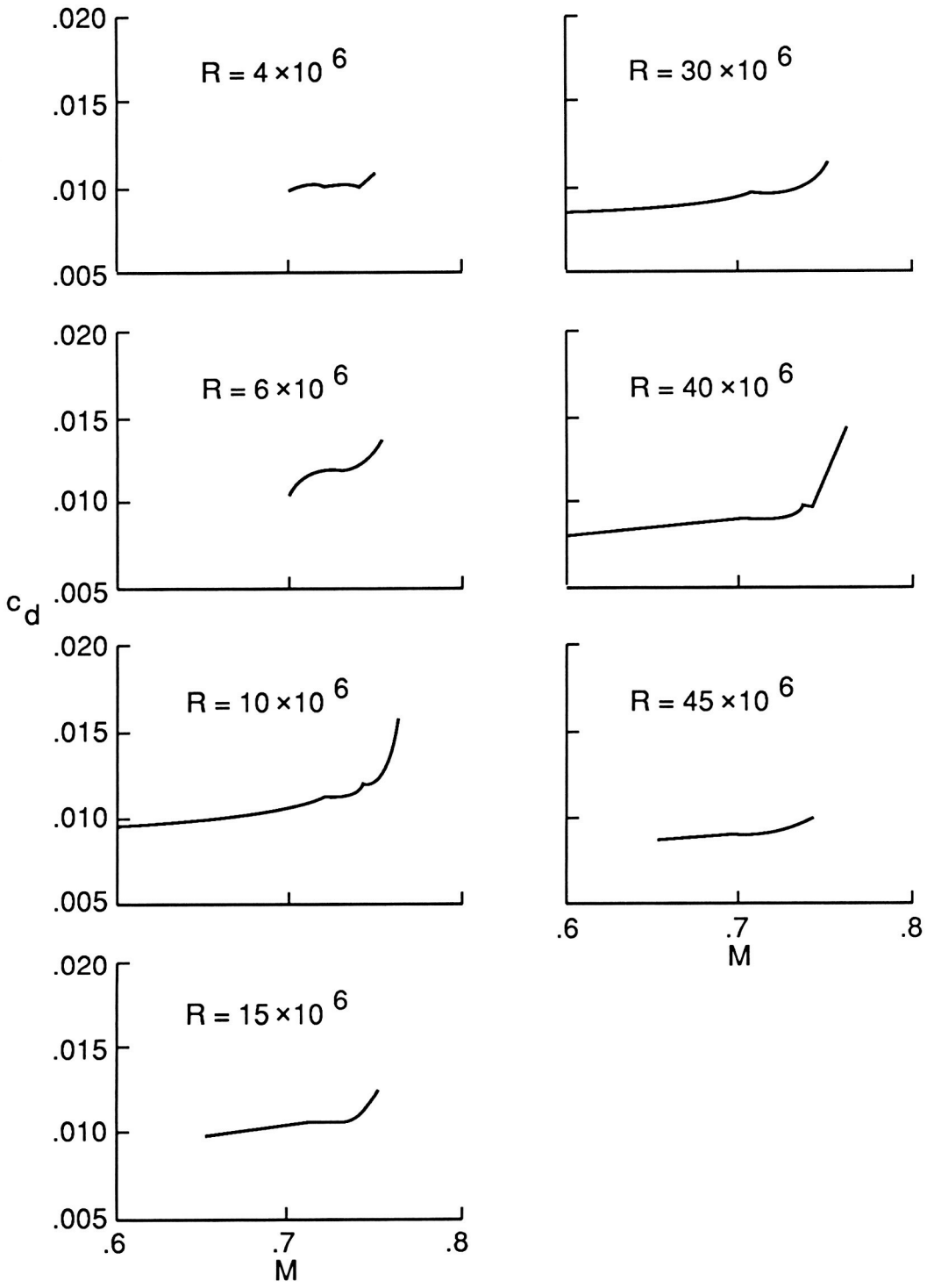

(e) $c_n = 0.70$.

Figure 4. Continued.

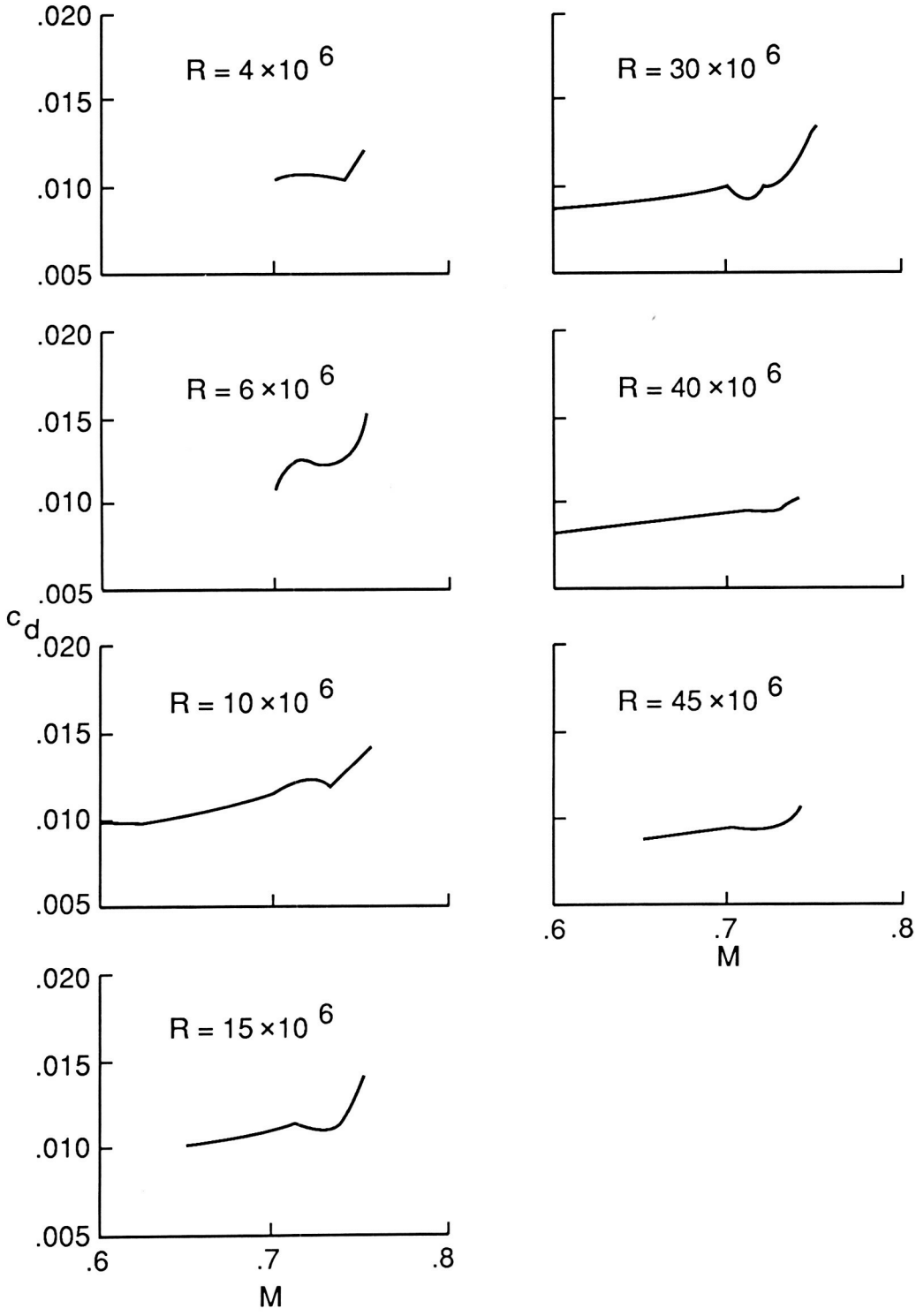

(f) $c_n = 0.75$.

Figure 4. Continued.

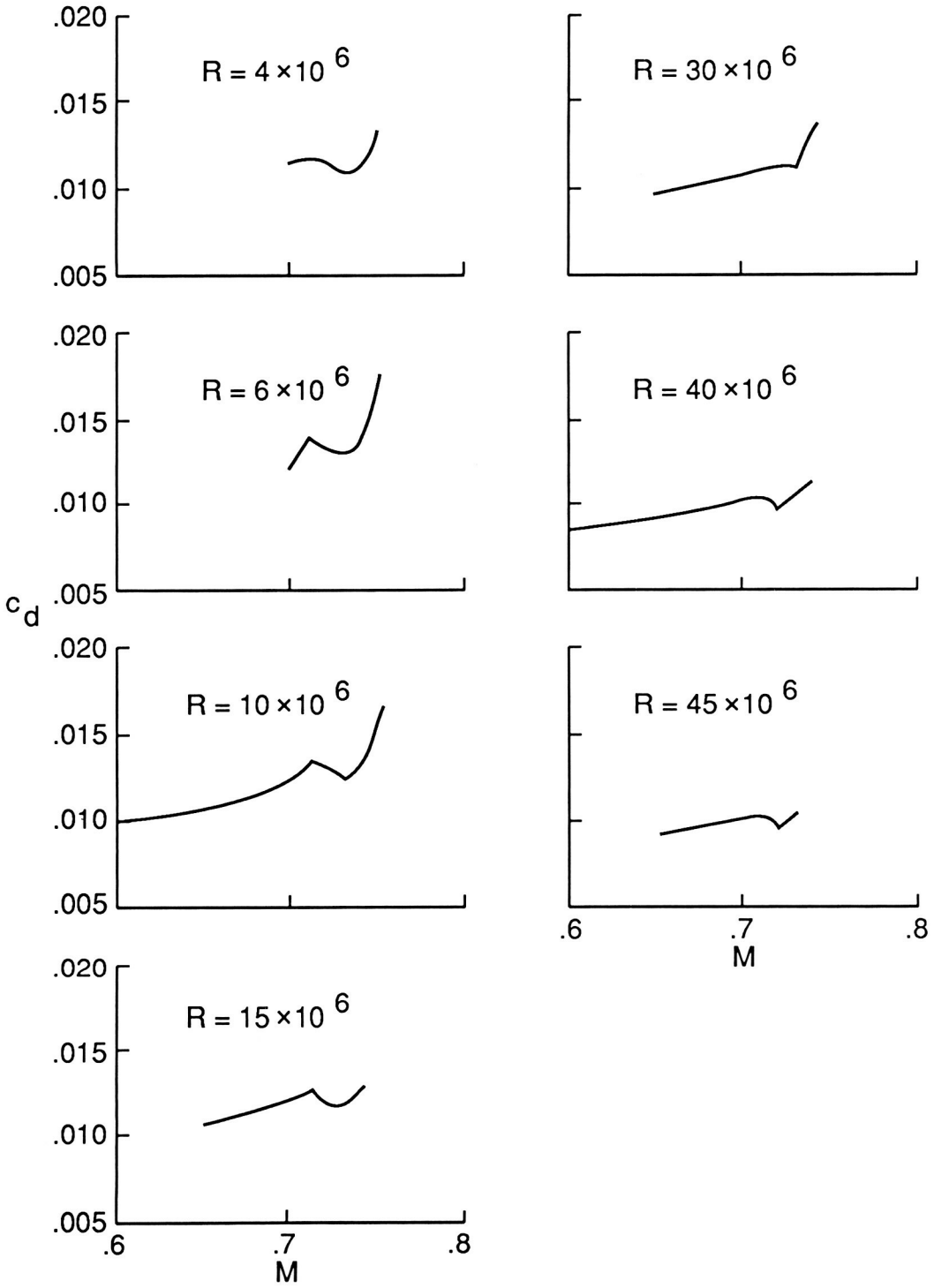

(g) $c_n = 0.80$.

Figure 4. Concluded.

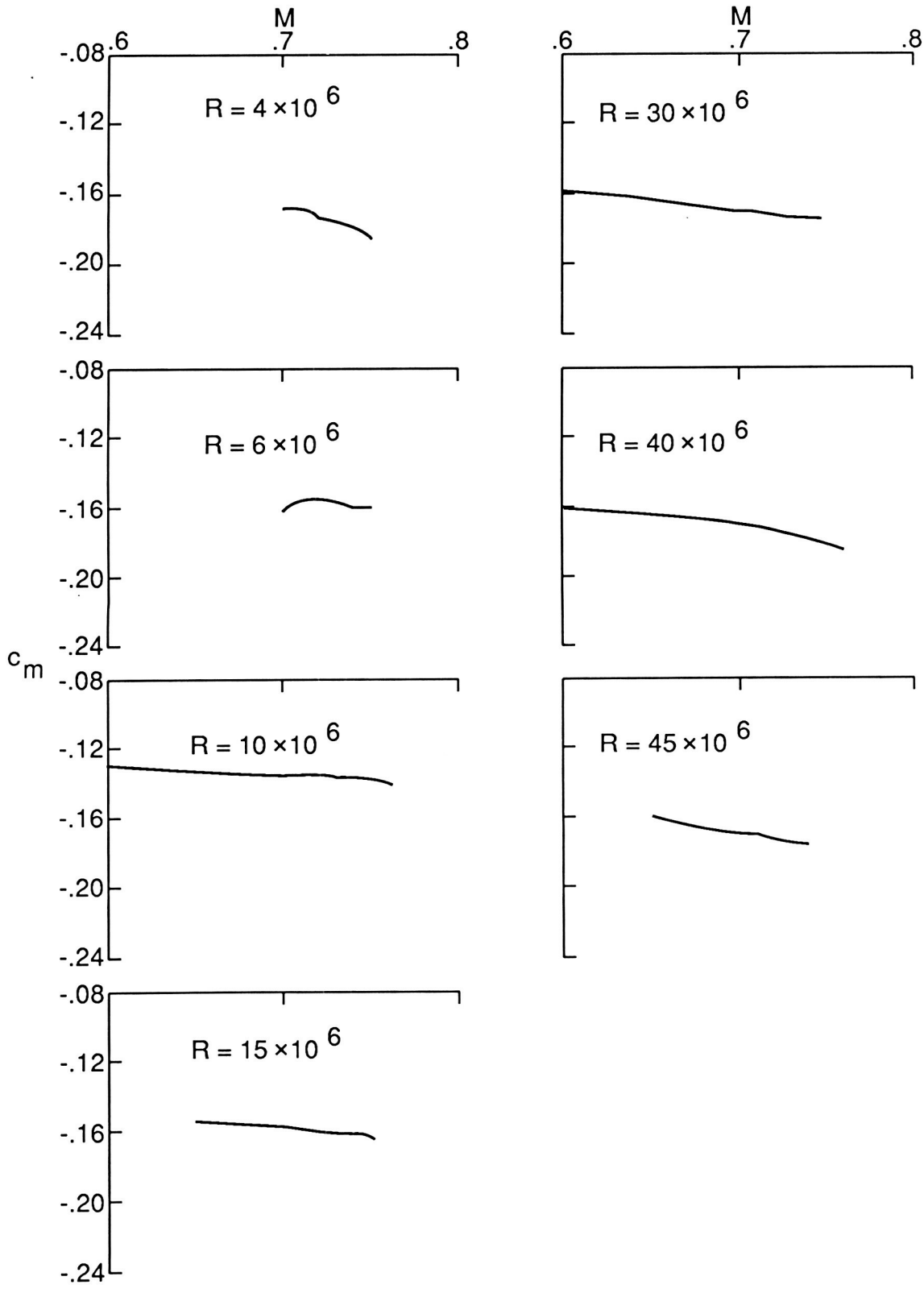

(a) $c_n = 0.50$.

Figure 5. Cross plots of quarter-chord pitching-moment coefficient versus Mach number at various normal-force coefficients. Uncorrected data.

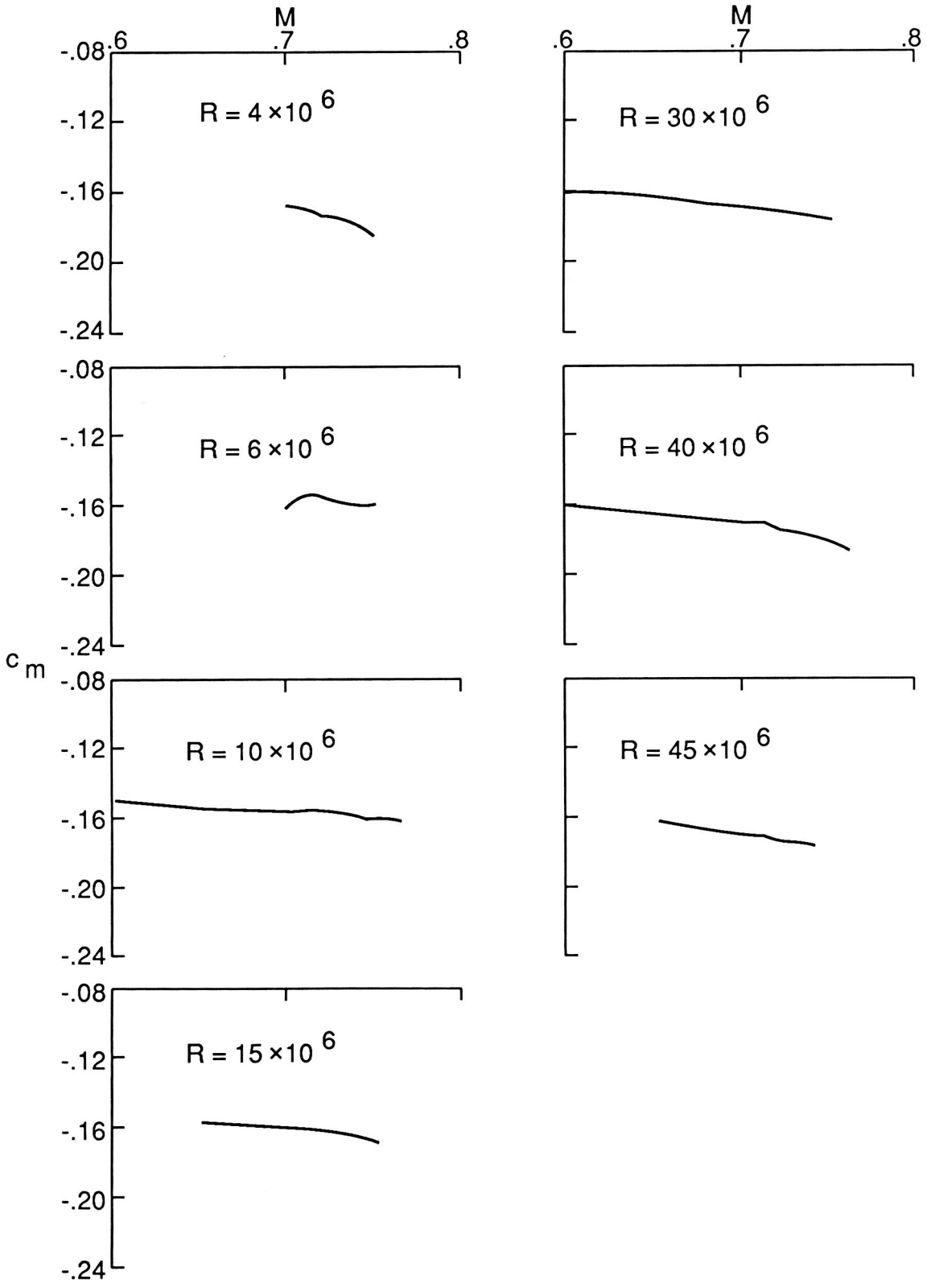

(b) $c_n = 0.55$.

Figure 5. Continued.

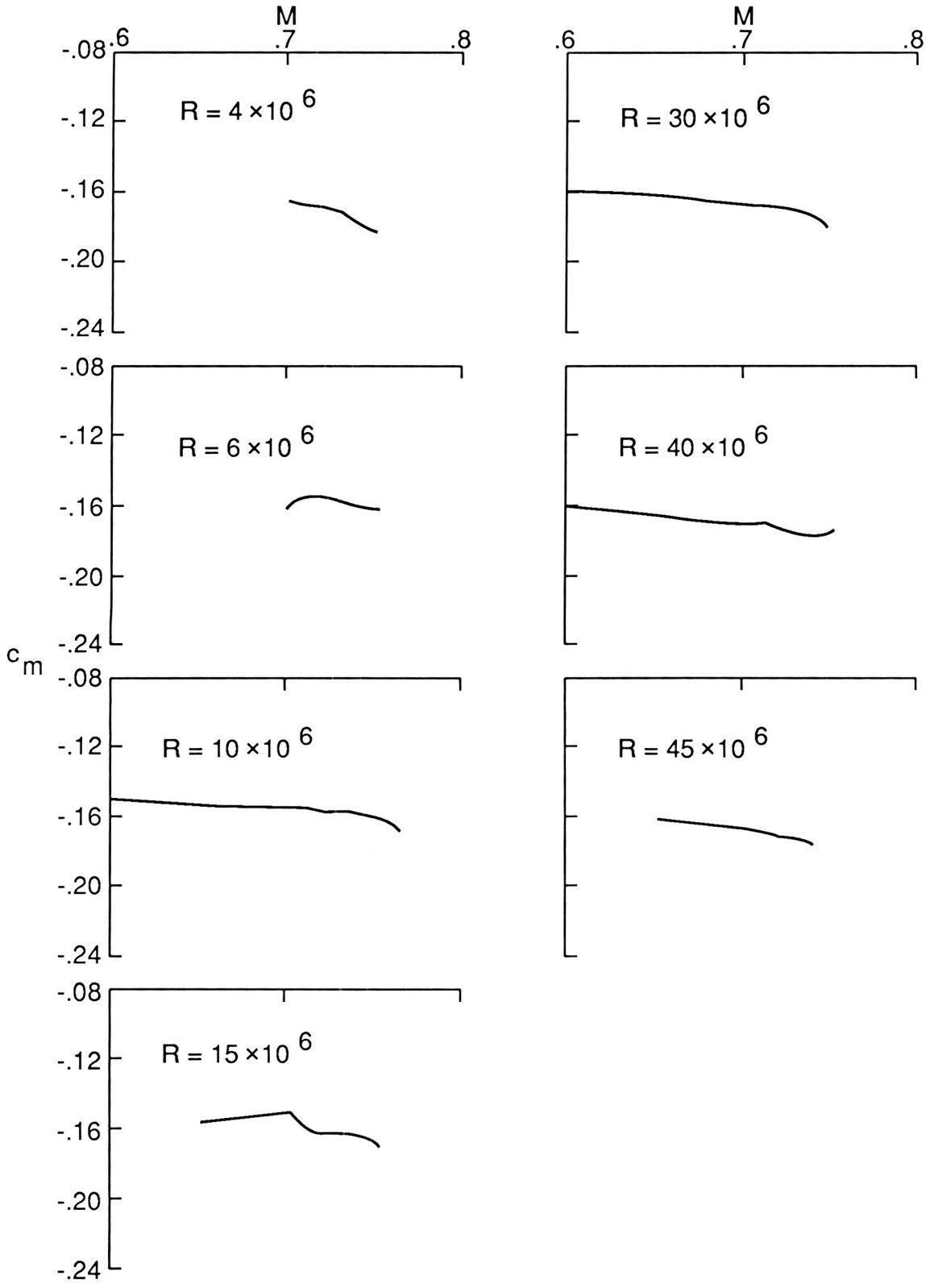

(c) $c_n = 0.60$.

Figure 5. Continued.

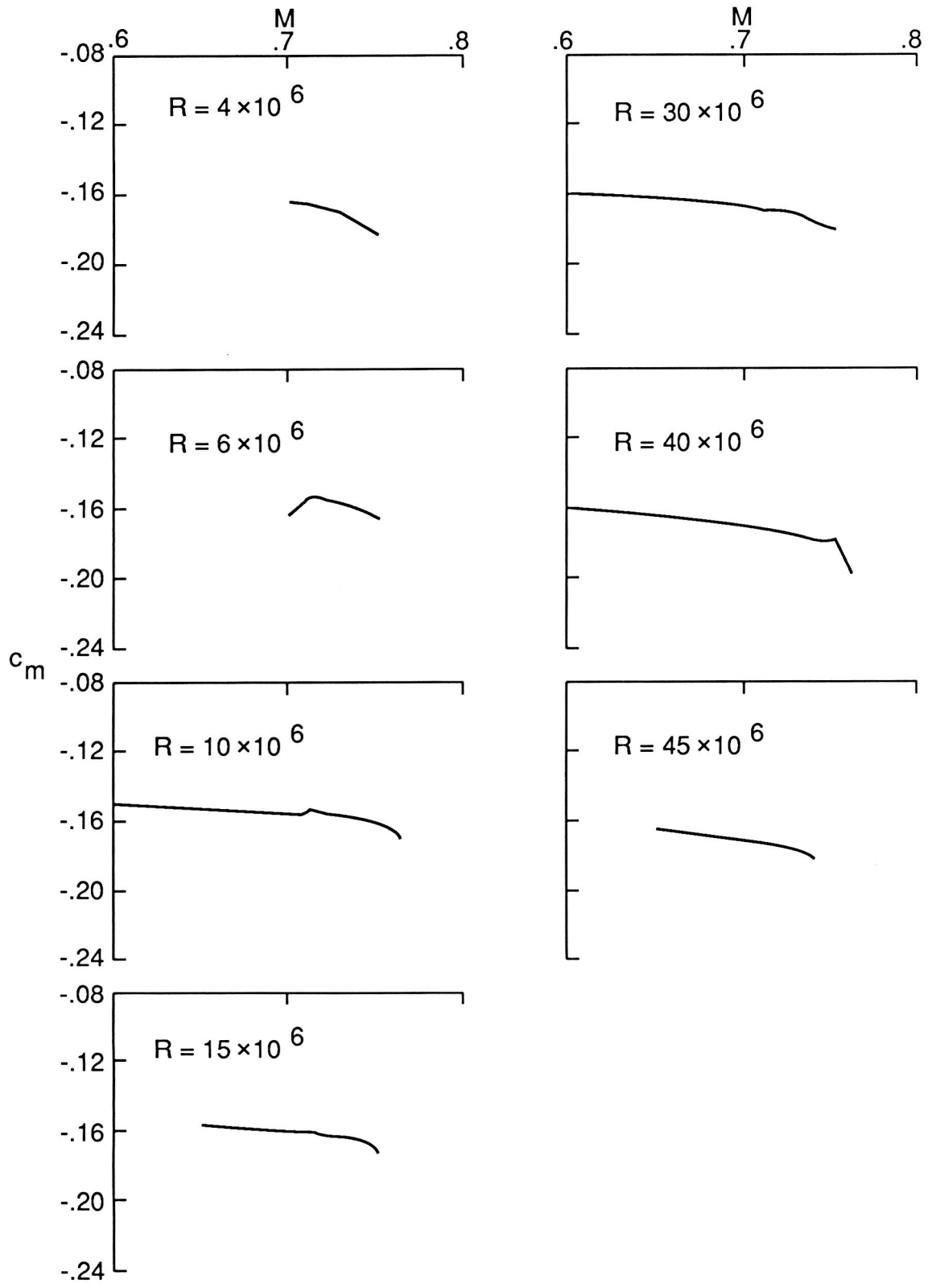

(d) $c_n = 0.65$.

Figure 5. Continued.

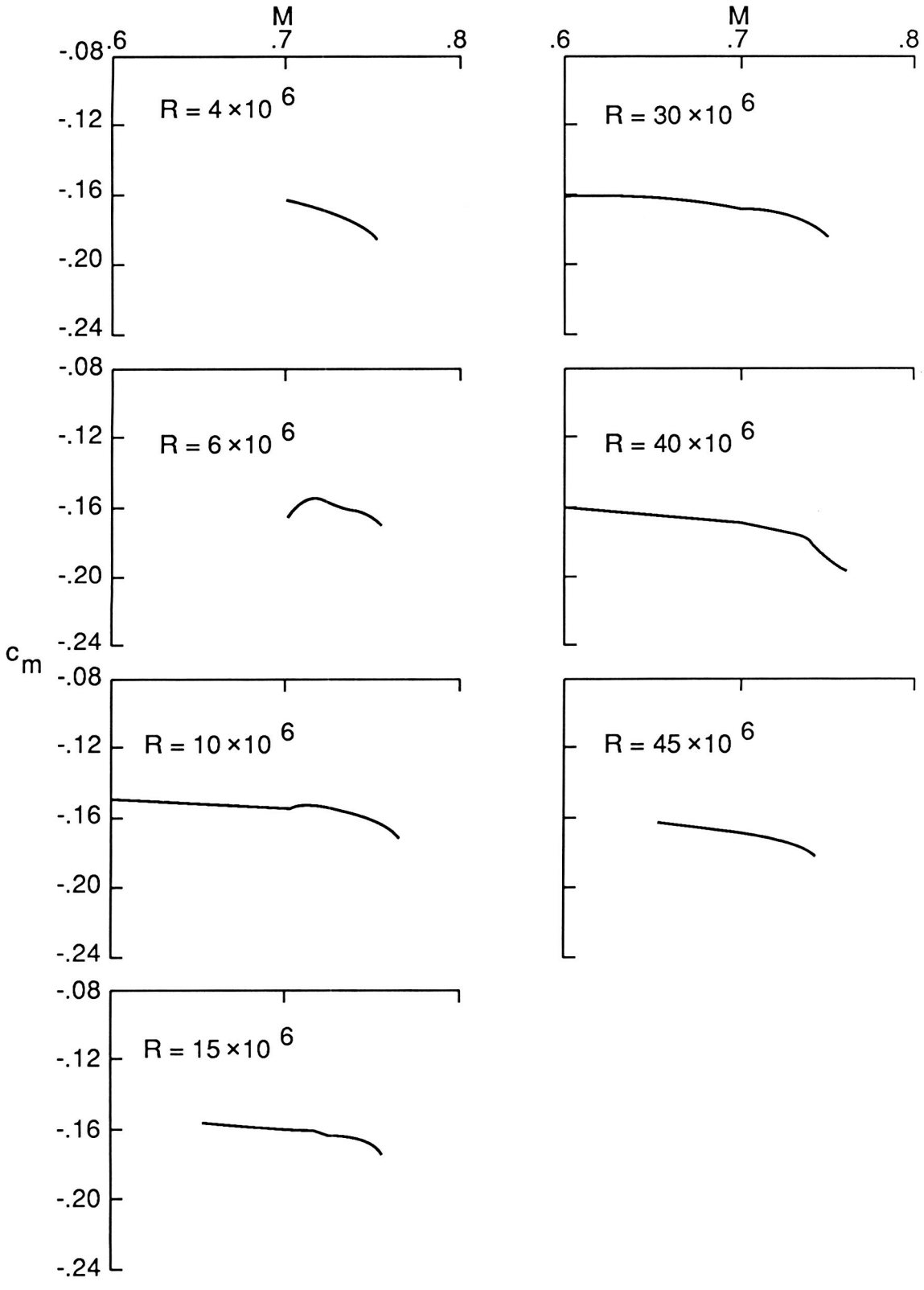

(e) $c_n = 0.70$.

Figure 5. Continued.

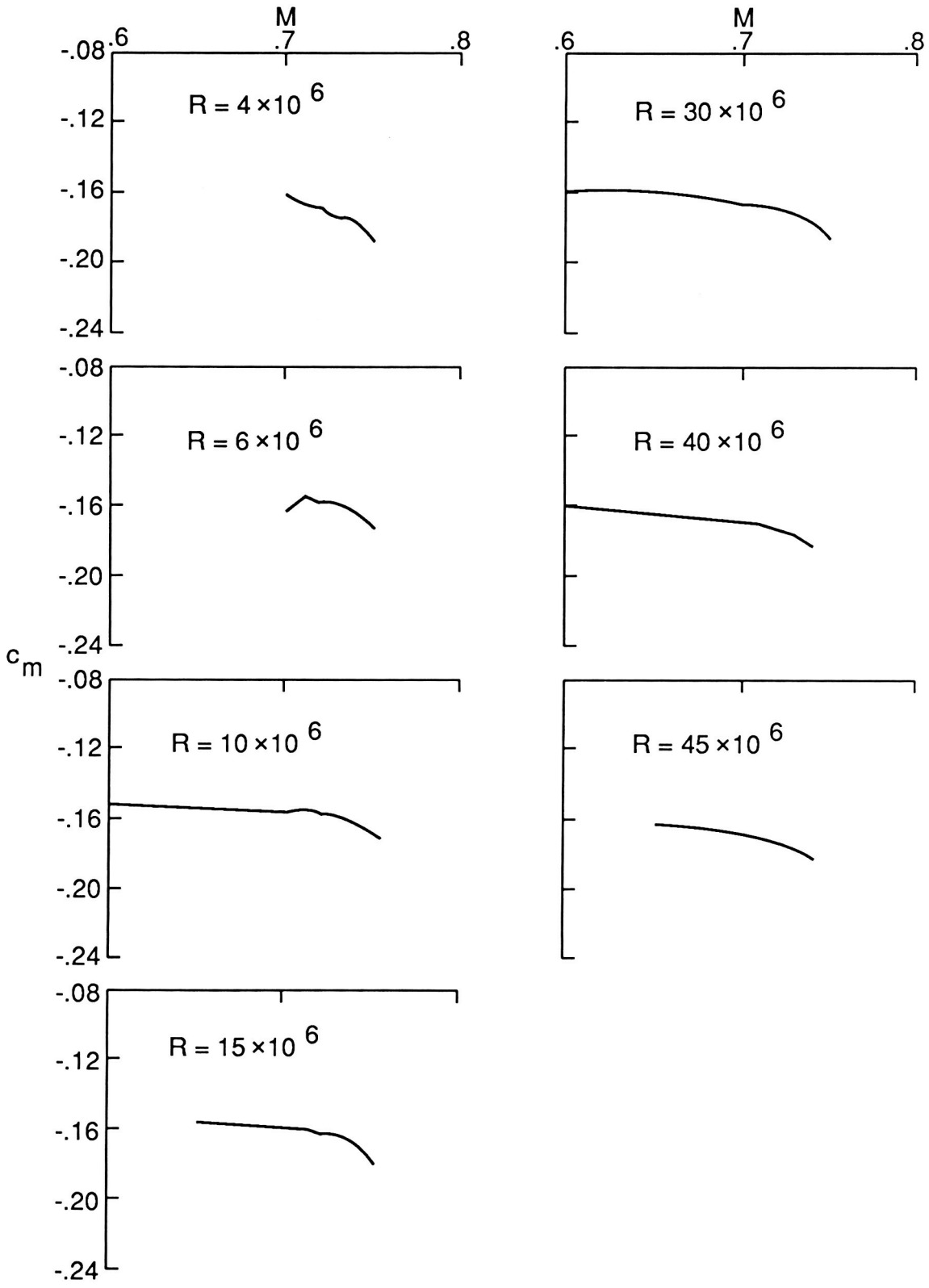

(f) $c_n = 0.75$.

Figure 5. Continued.

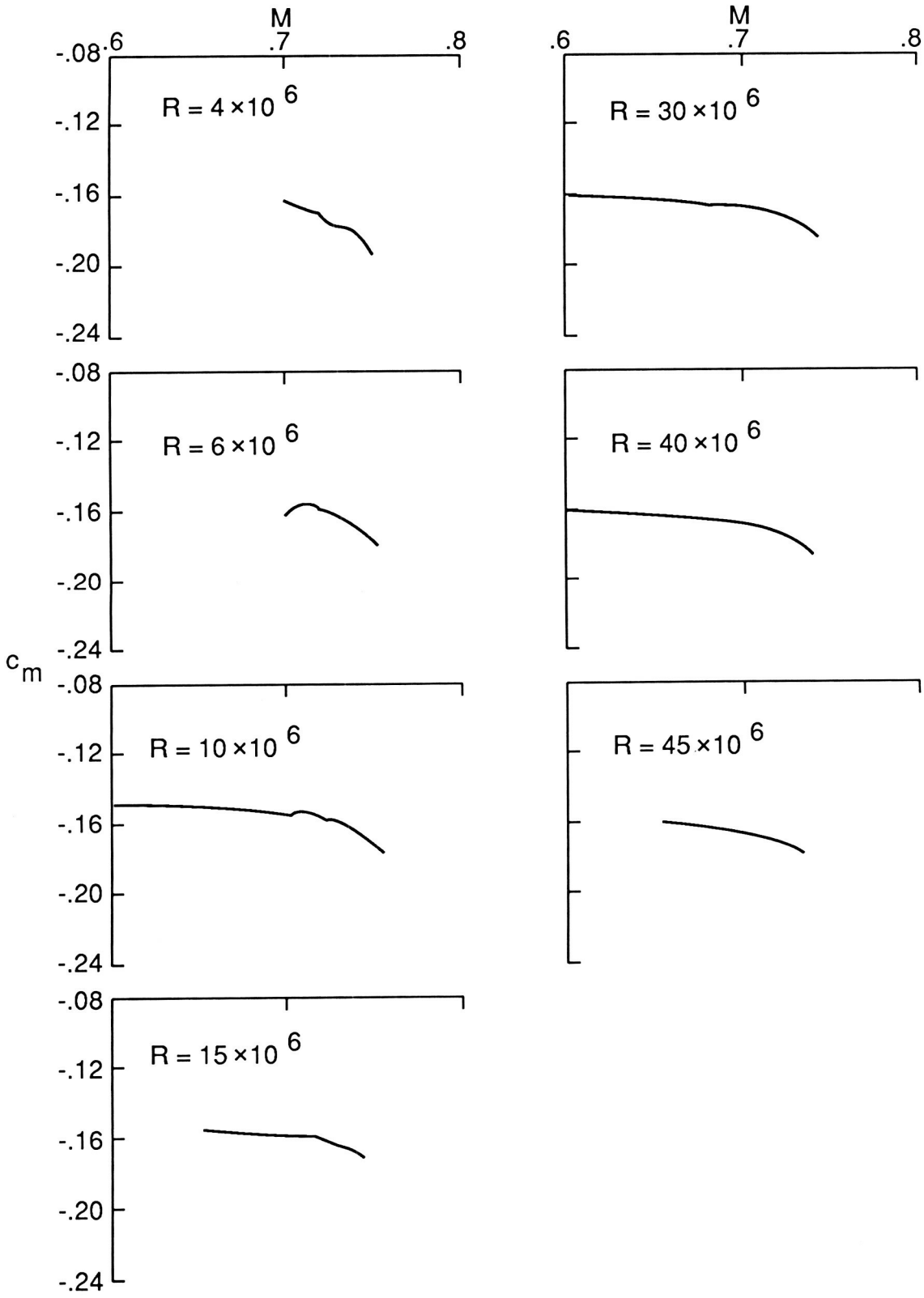

(g) $c_n = 0.80$.

Figure 5. Concluded.

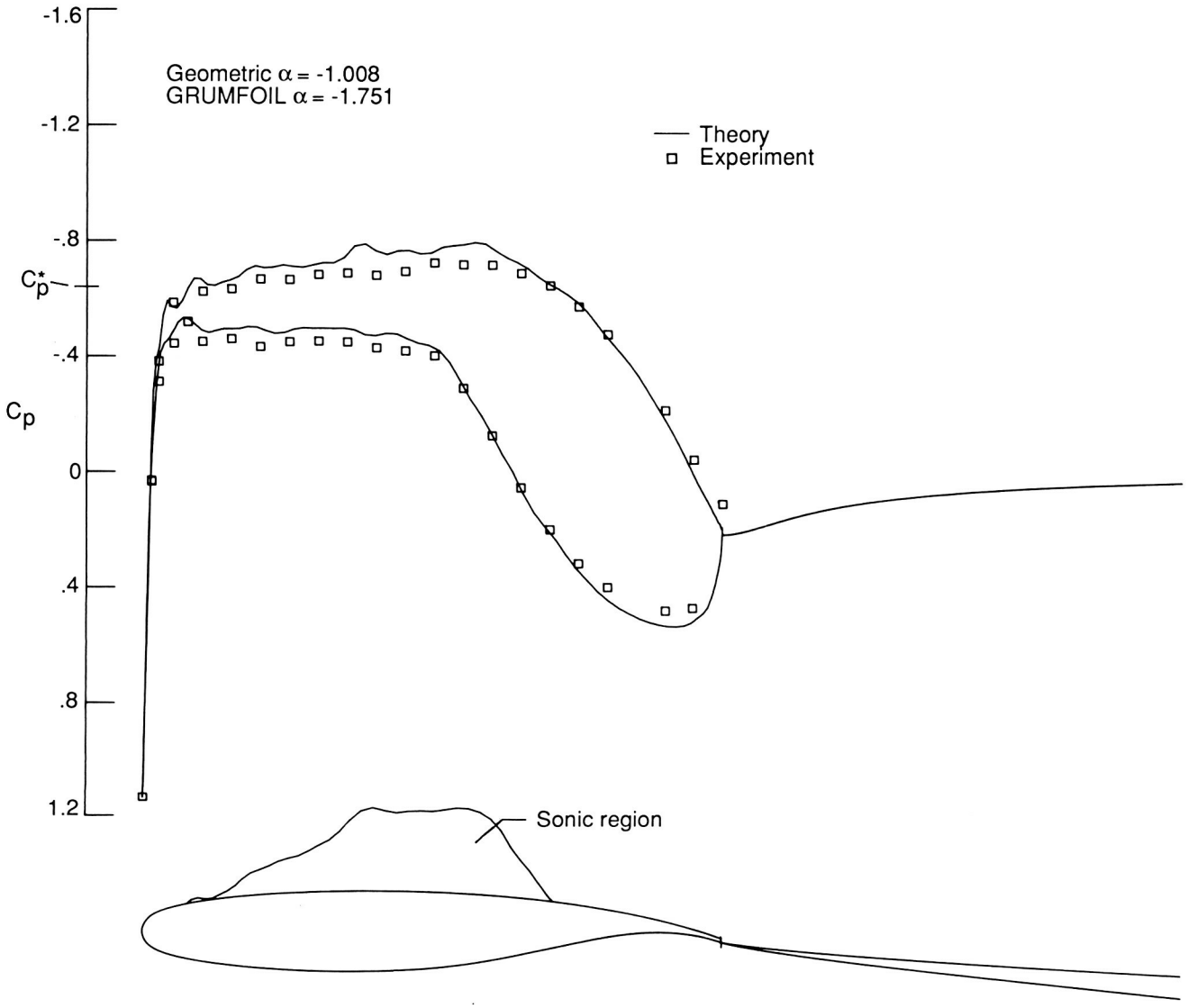

Figure 6. Uncorrected data compared with theoretical results at low lift. $M = 0.736$; $c_n = 0.4425$; $R = 40 \times 10^6$.

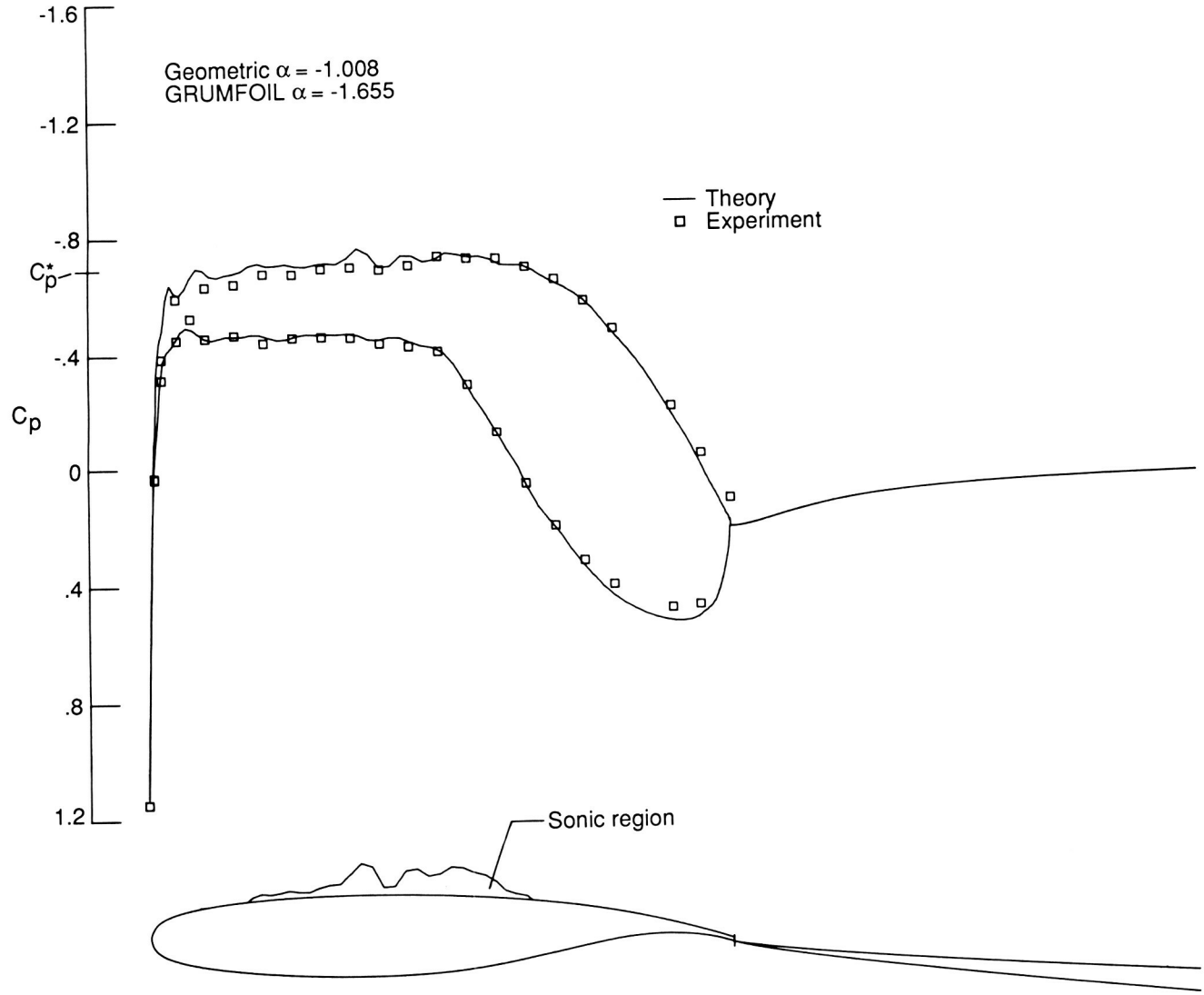

Figure 7. Data corrected for sidewalls only compared with theoretical results at low lift. $M = 0.722$; $c_n = 0.4483$; $R = 40 \times 10^6$.

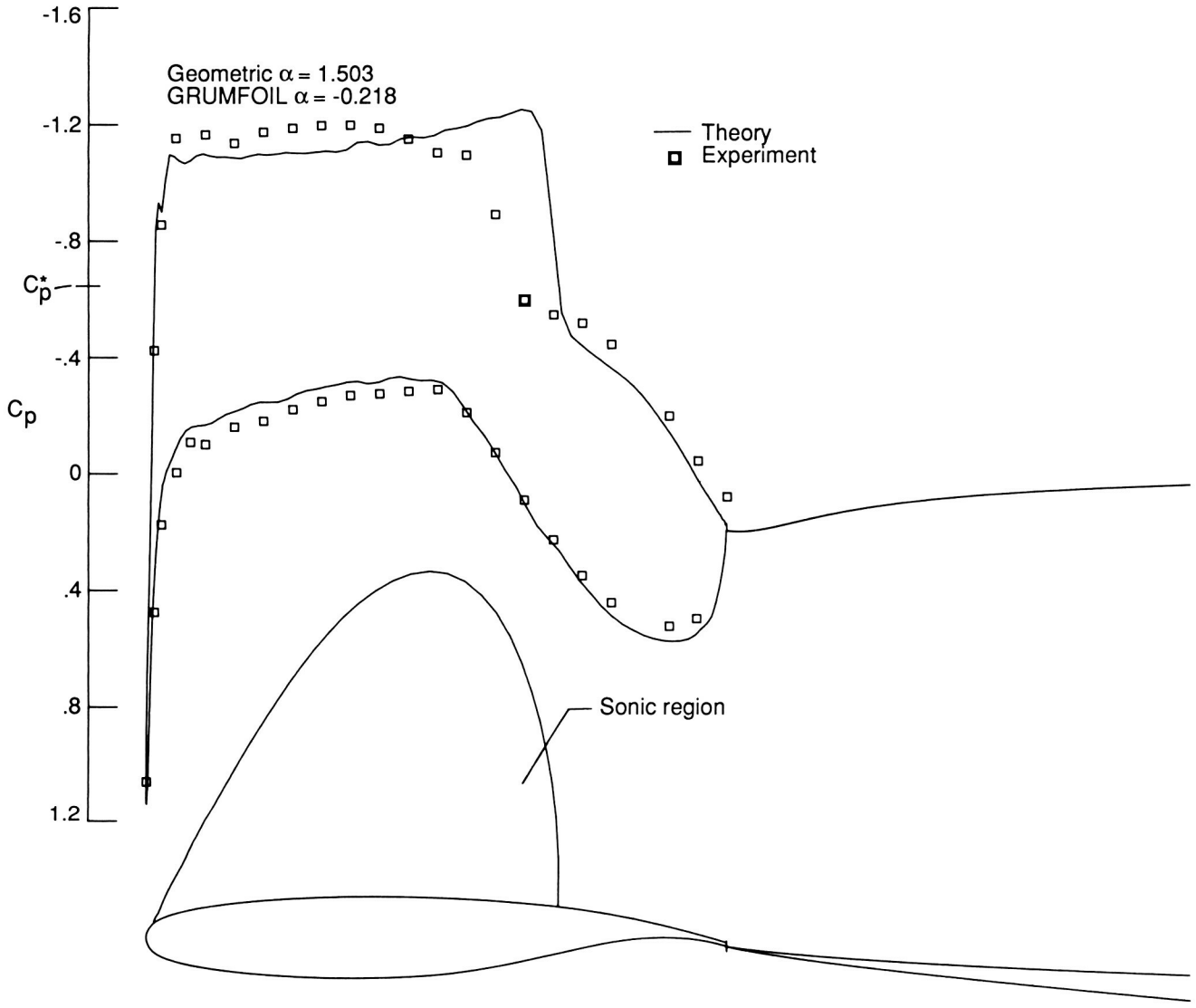

Figure 8. Uncorrected data compared with theoretical results at high lift. $M = 0.735$; $c_n = 0.8598$; $R = 40 \times 10^6$.

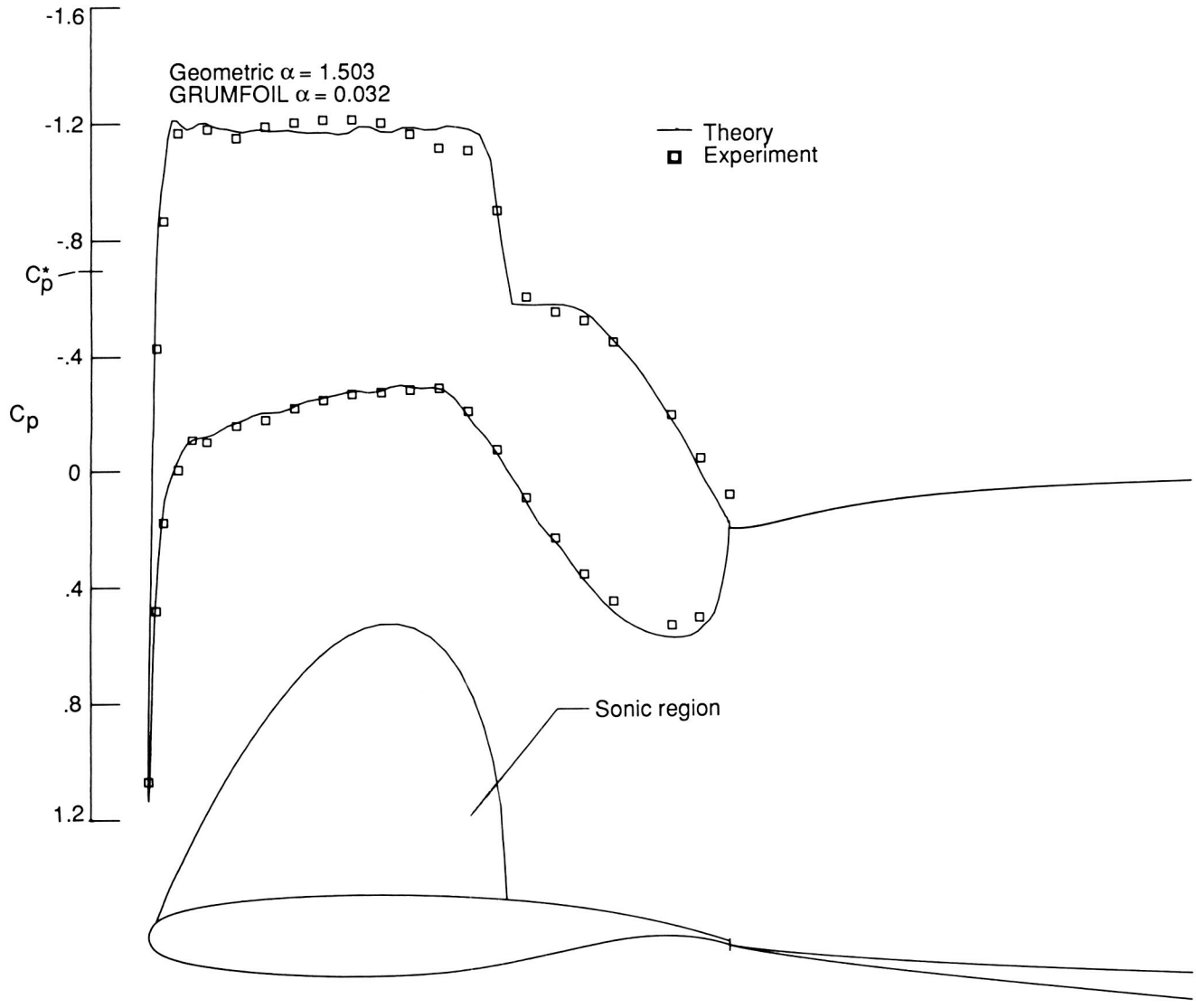

Figure 9. Data corrected for sidewalls only compared with theoretical results at high lift. $M = 0.721$; $c_n = 0.8710$; $R = 40 \times 10^6$.

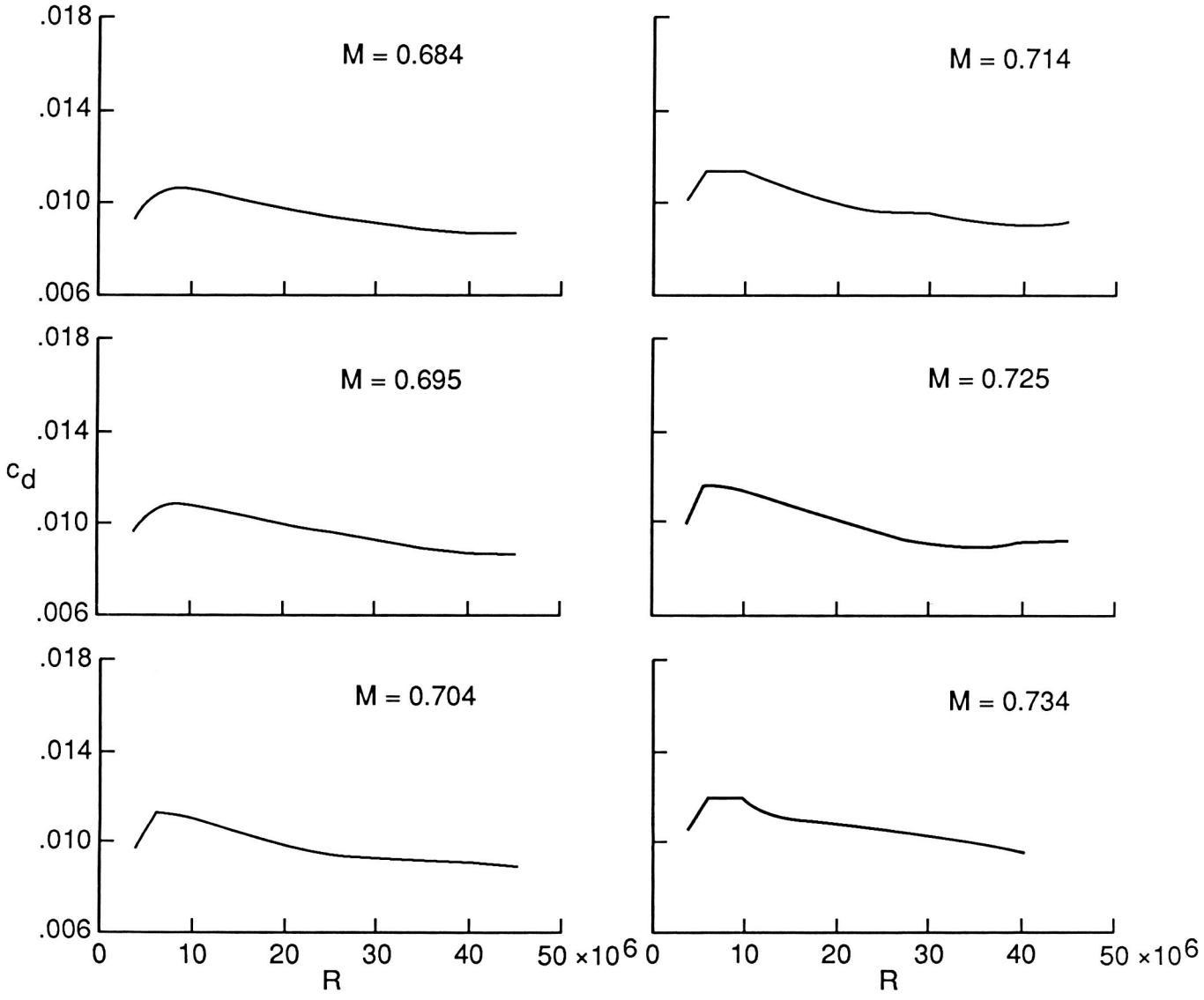

(a) $c_n = 0.51$.

Figure 10. Profile-drag coefficient versus Reynolds number at various normal-force coefficients. Data corrected using the tables of reference 14.

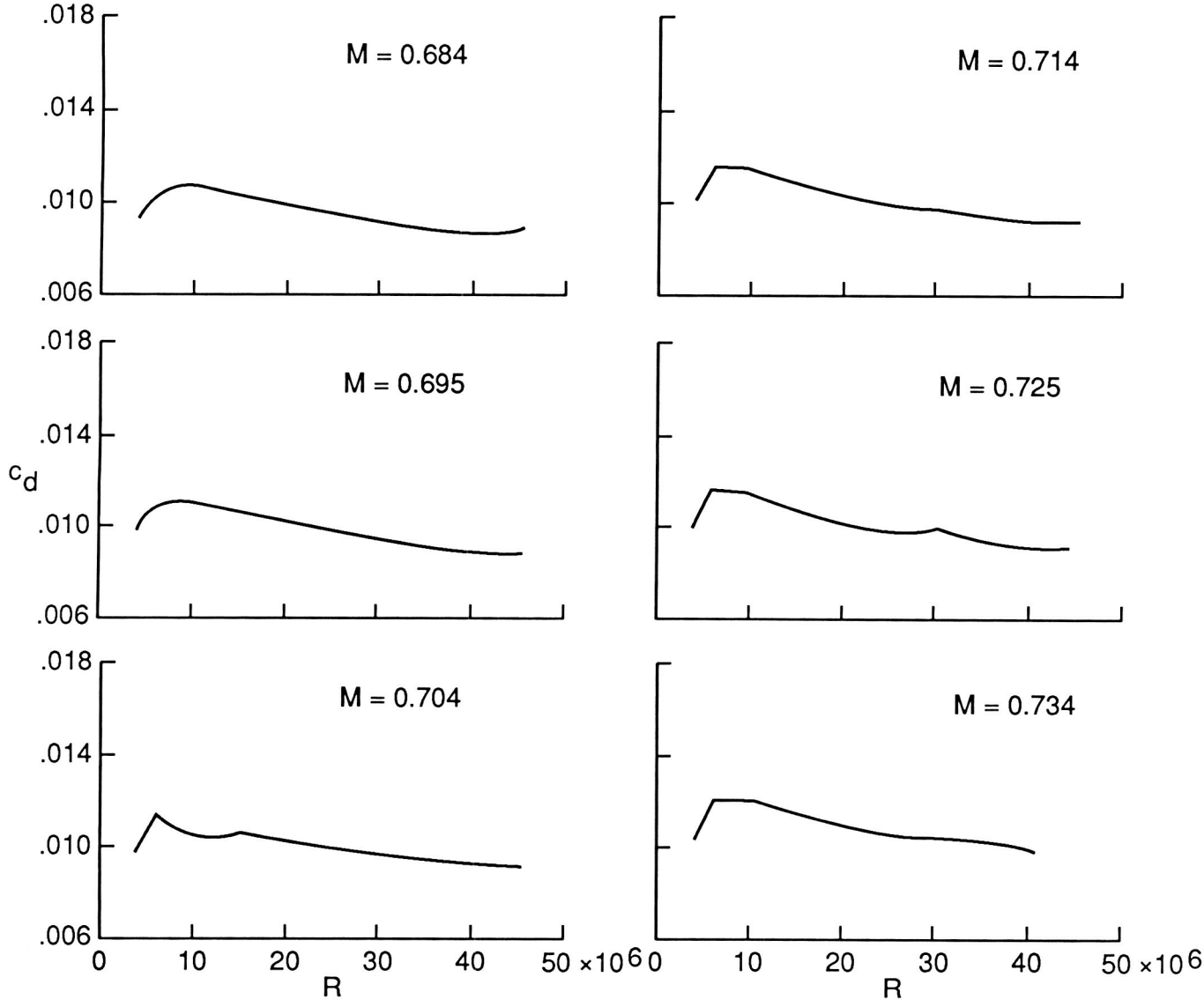

(b) $c_n = 0.56$.

Figure 10. Continued.

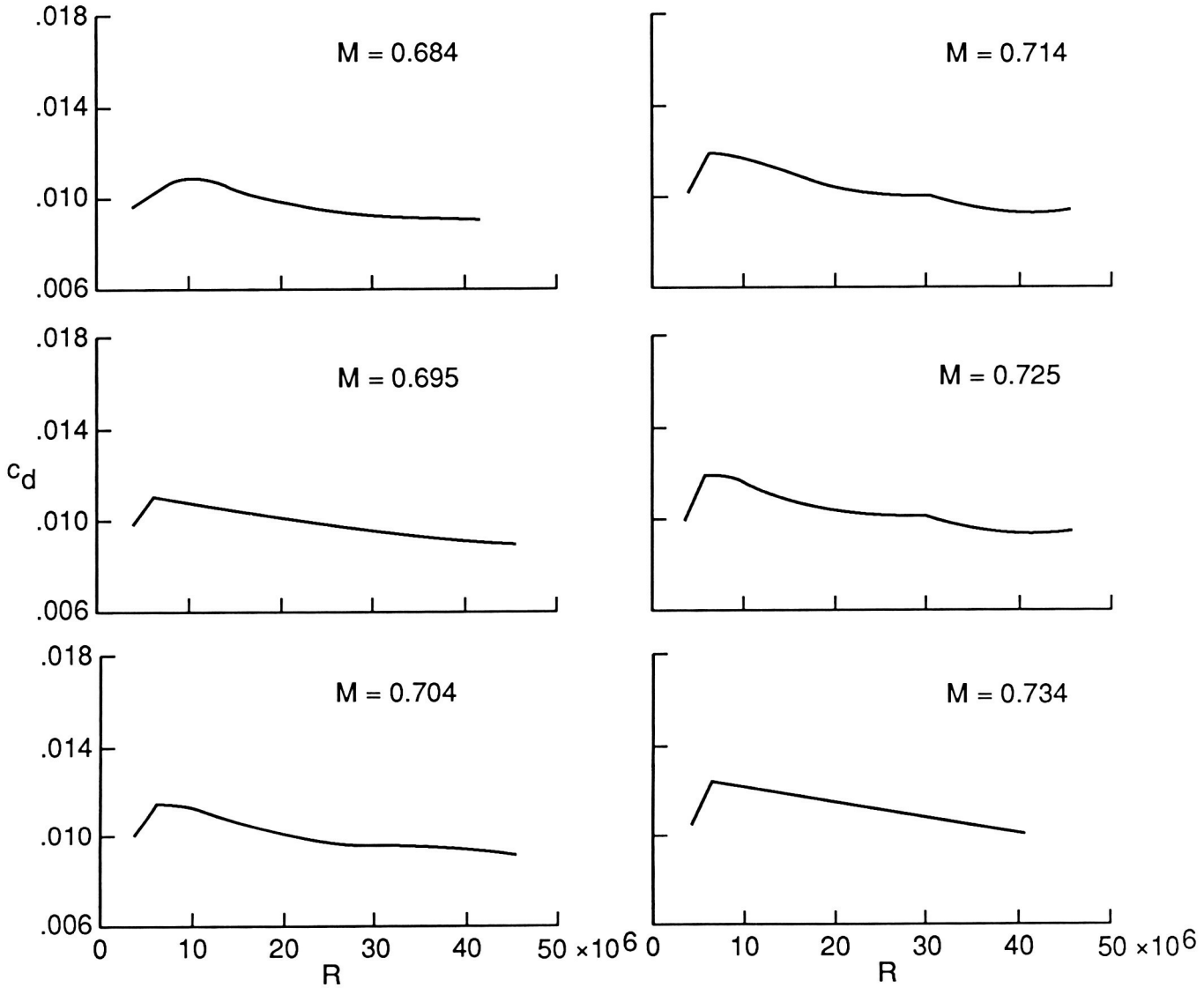

(c) $c_n = 0.61$.

Figure 10. Continued.

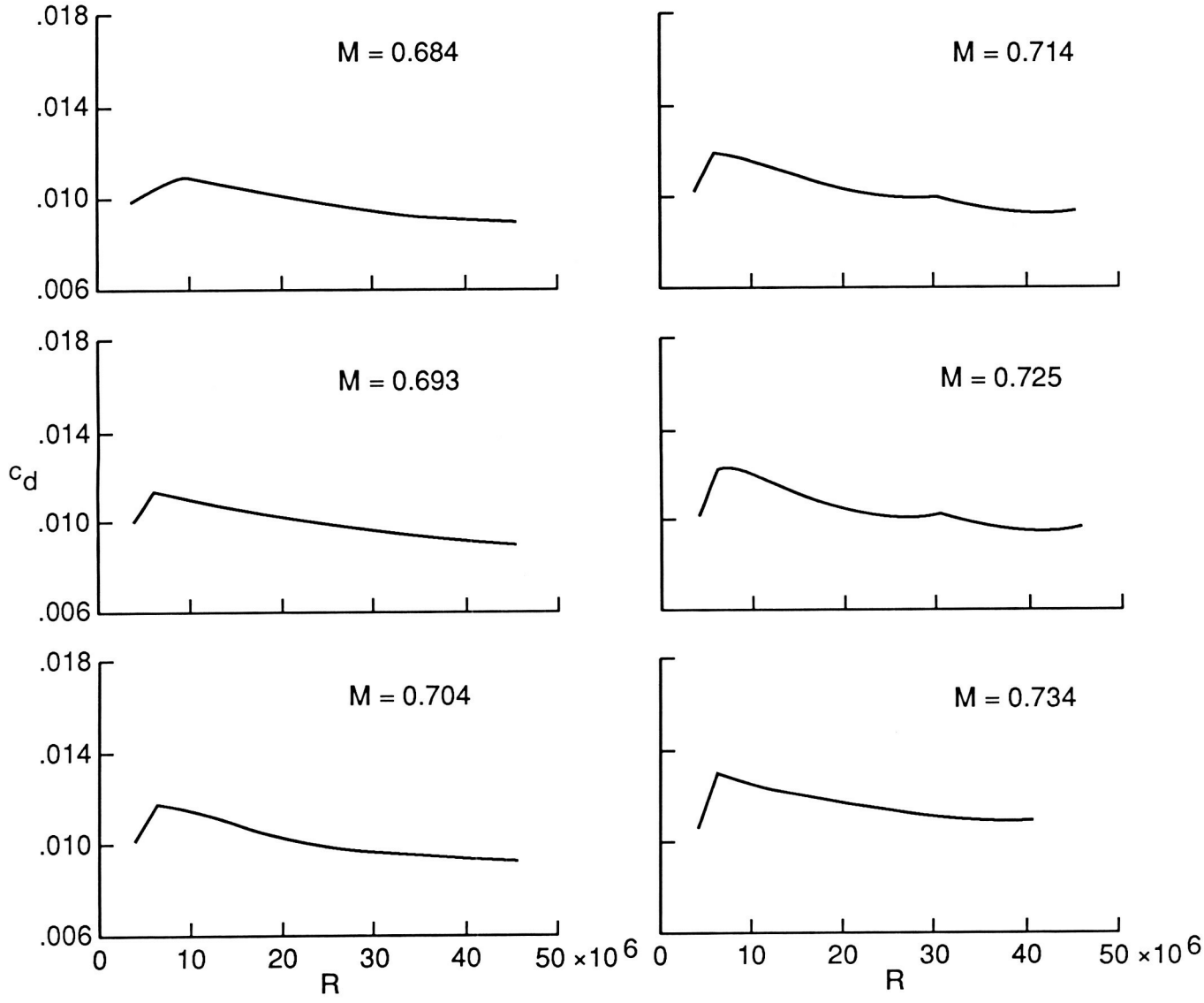

(d) $c_n = 0.66$.

Figure 10. Continued.

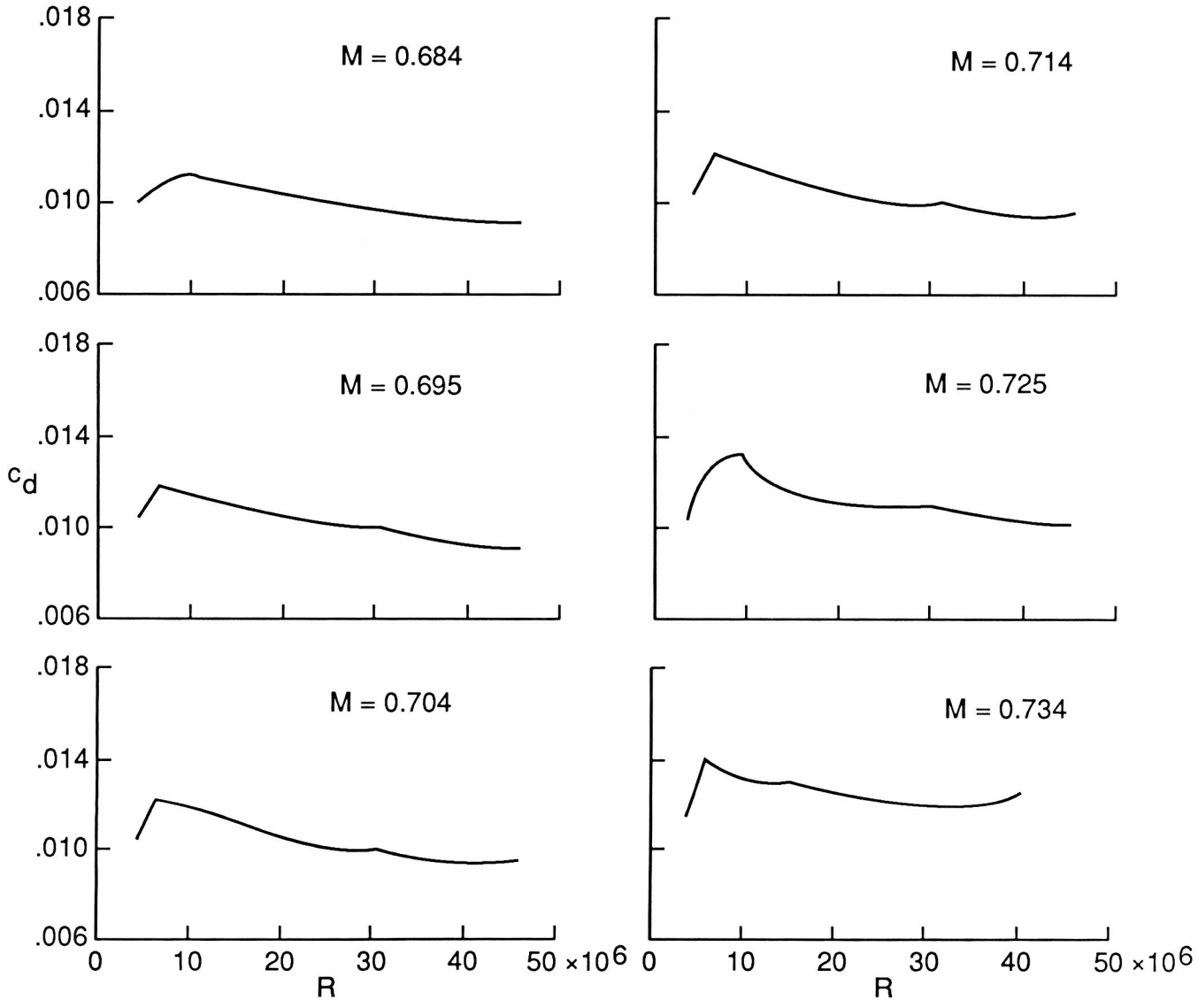

(e) $c_n = 0.71$.

Figure 10. Continued.

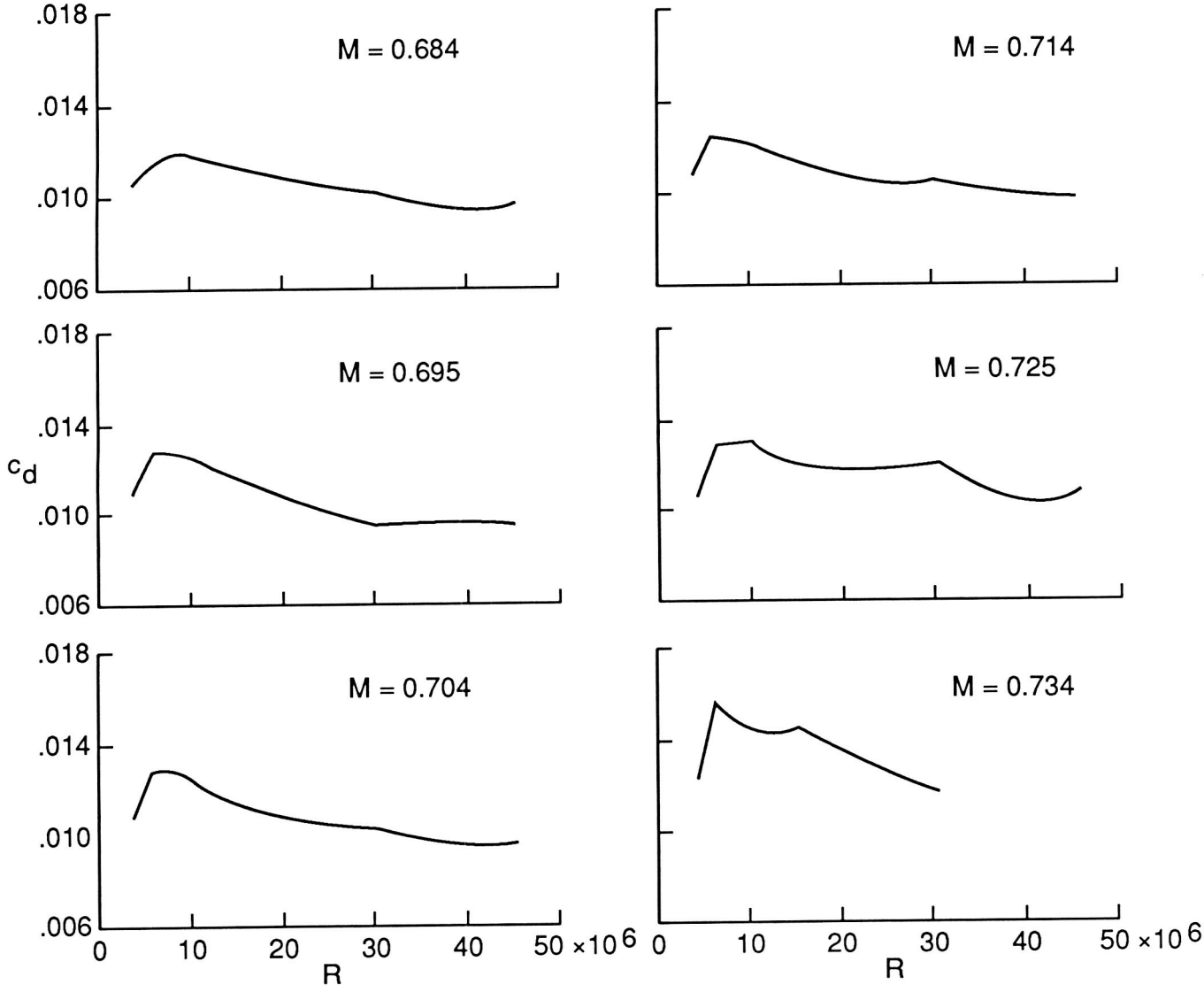

(f) $c_n = 0.76$.

Figure 10. Continued.

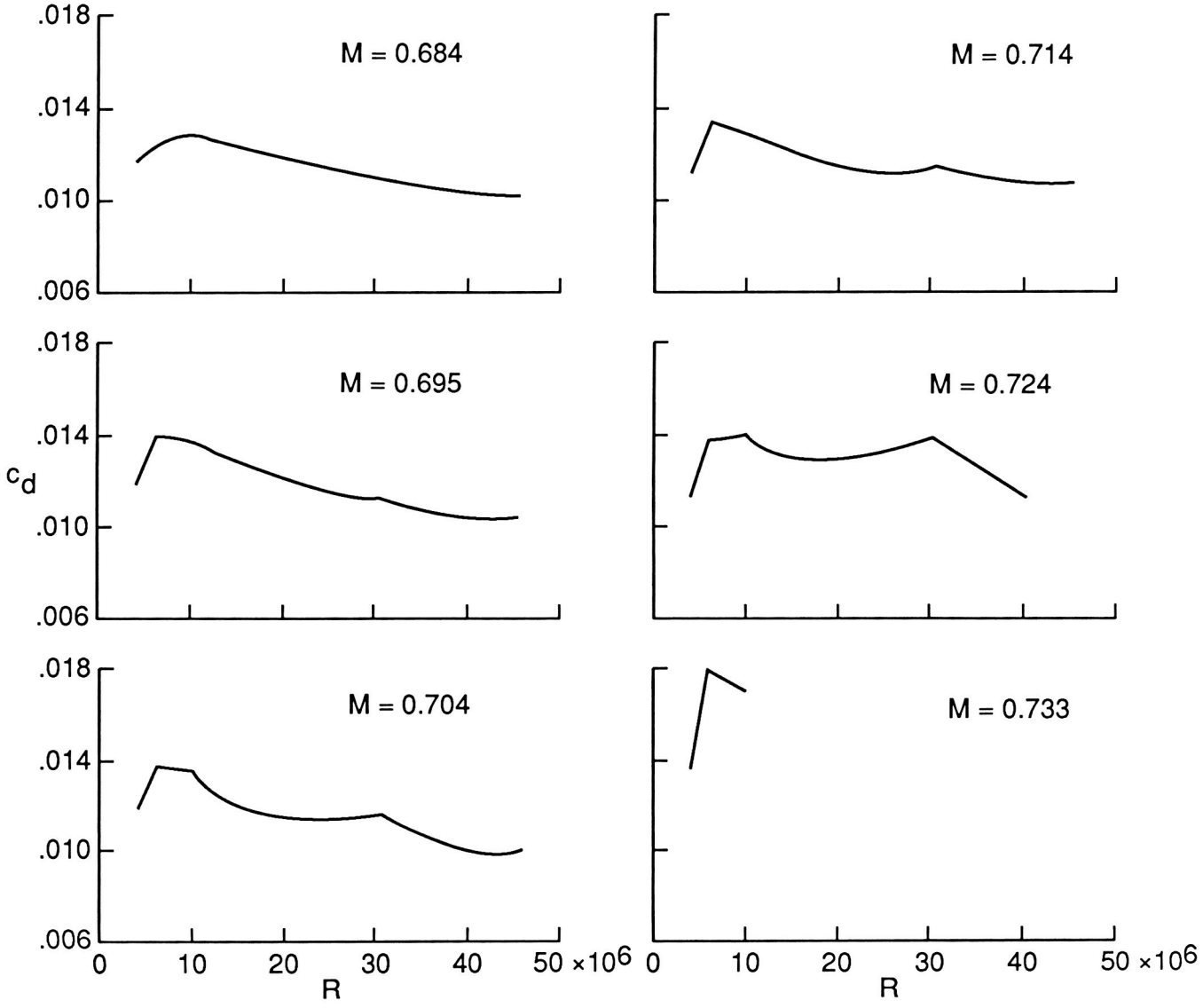

(g) $c_n = 0.81$.

Figure 11. Concluded.

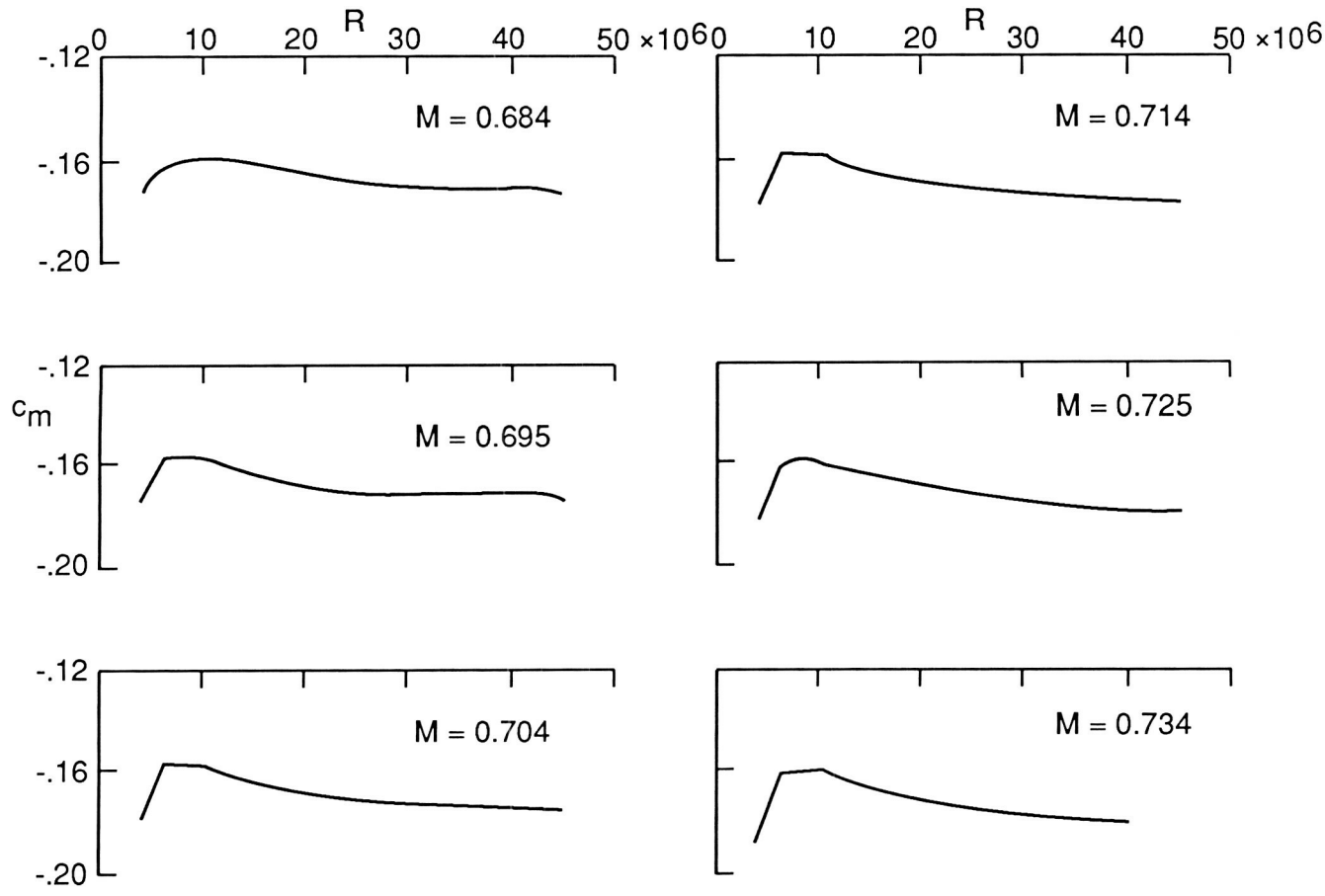

(a) $c_n = 0.51$.

Figure 11. Quarter-chord pitching-moment coefficient versus Reynolds number at various normal-force coefficients. Data corrected using the tables of reference 14.

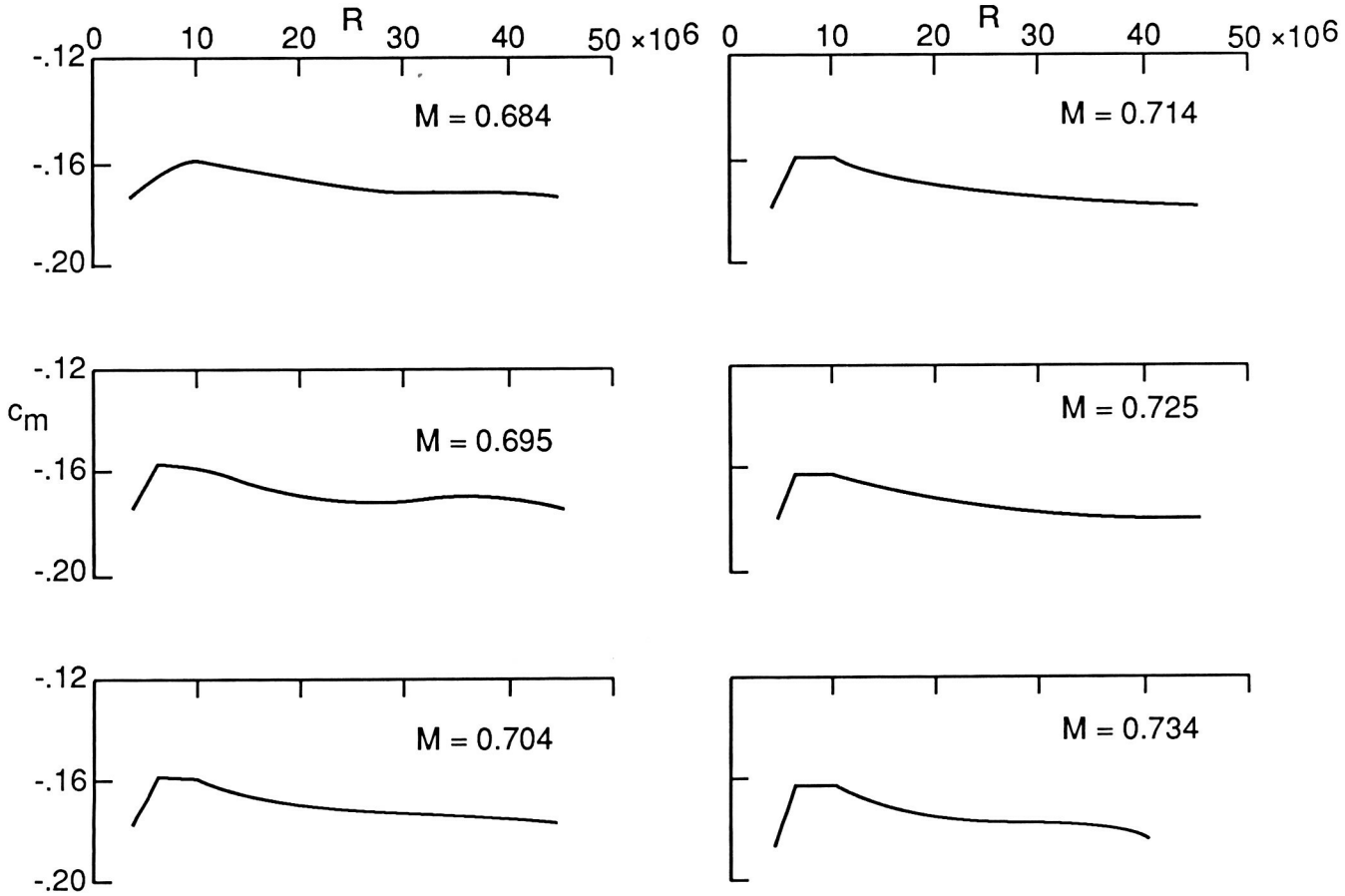

(b) $c_n = 0.56$.

Figure 11. Continued.

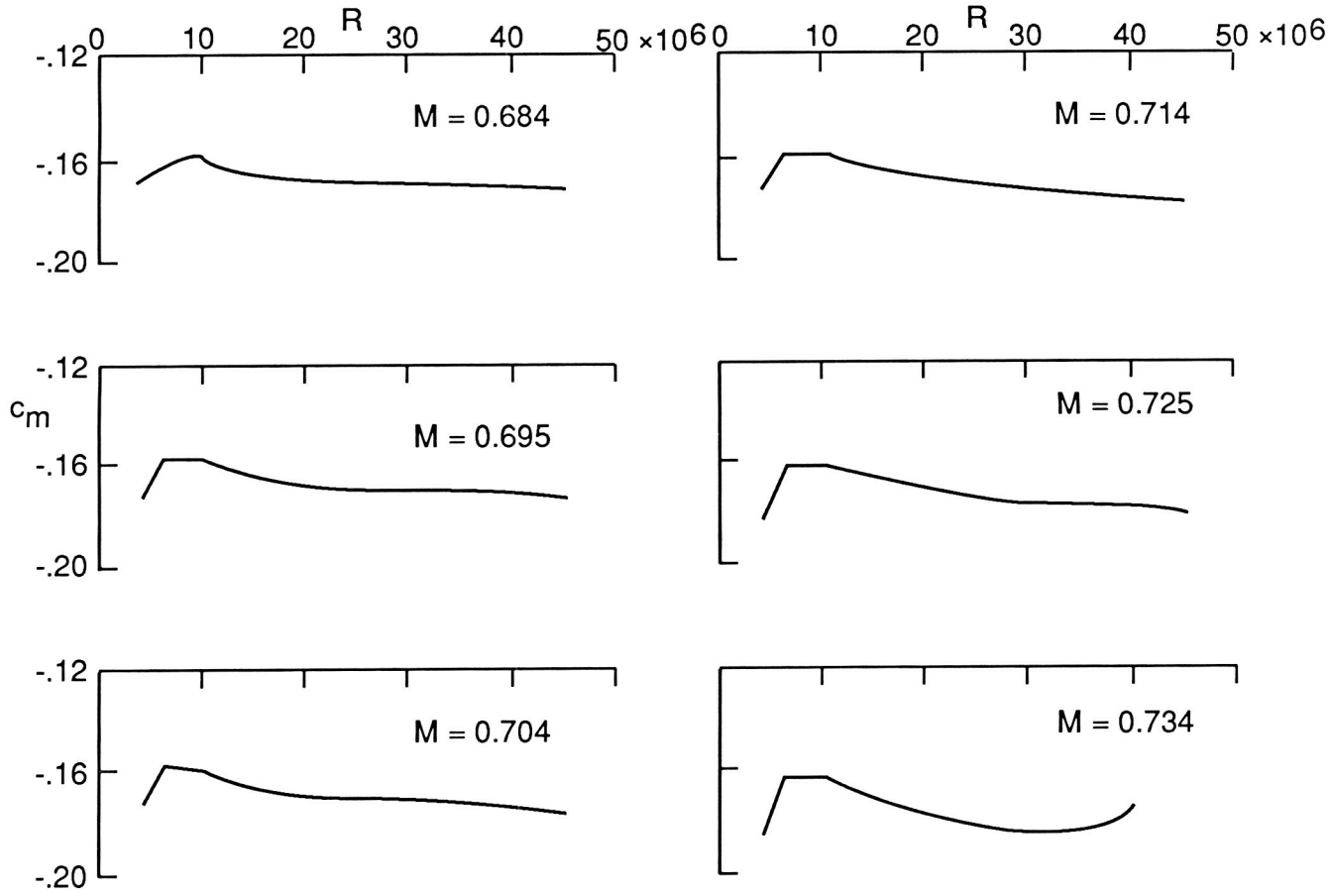

(c) $c_n = 0.61$.

Figure 11. Continued.

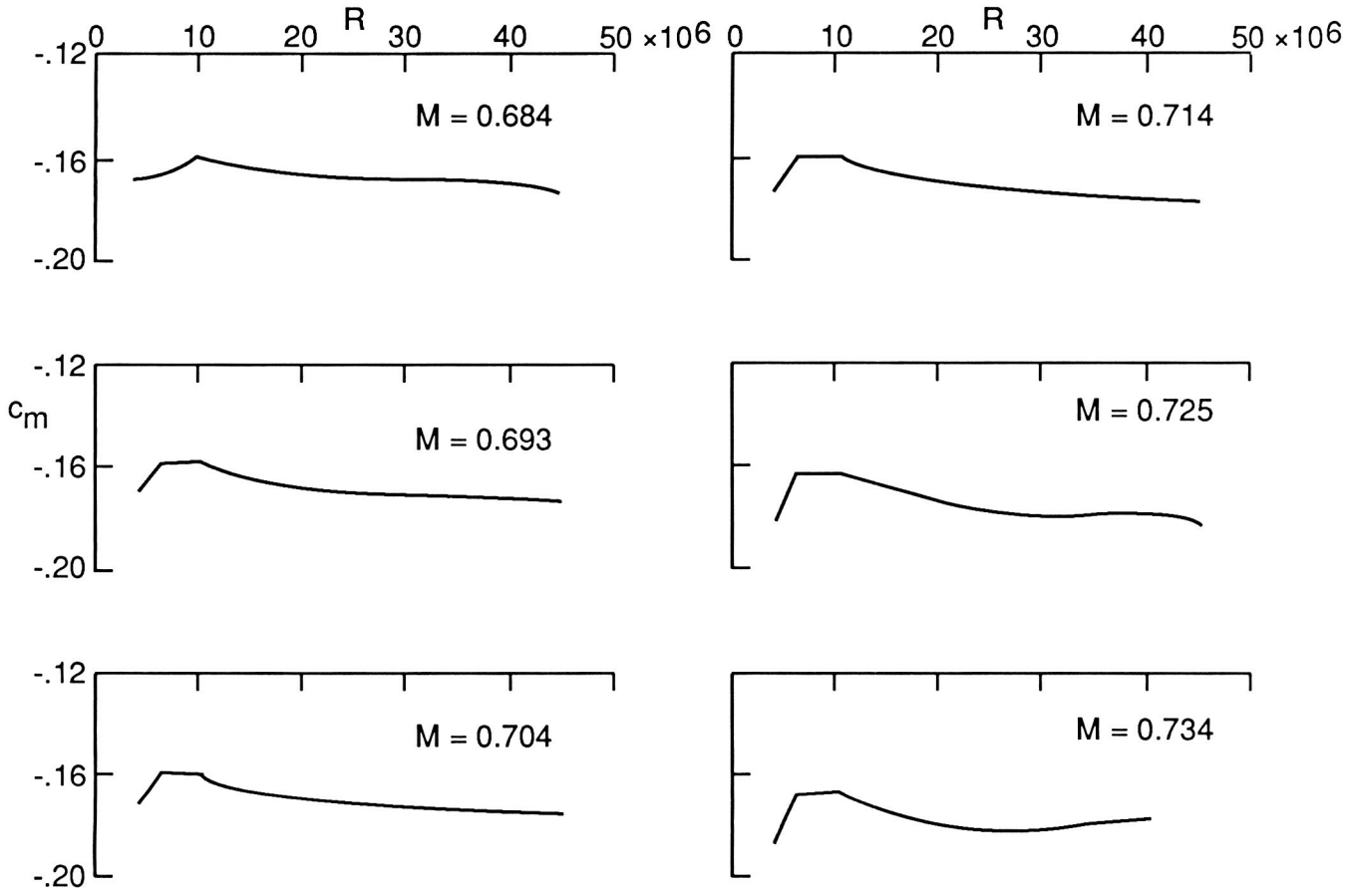

(d) $c_n = 0.66$.

Figure 11. Continued.

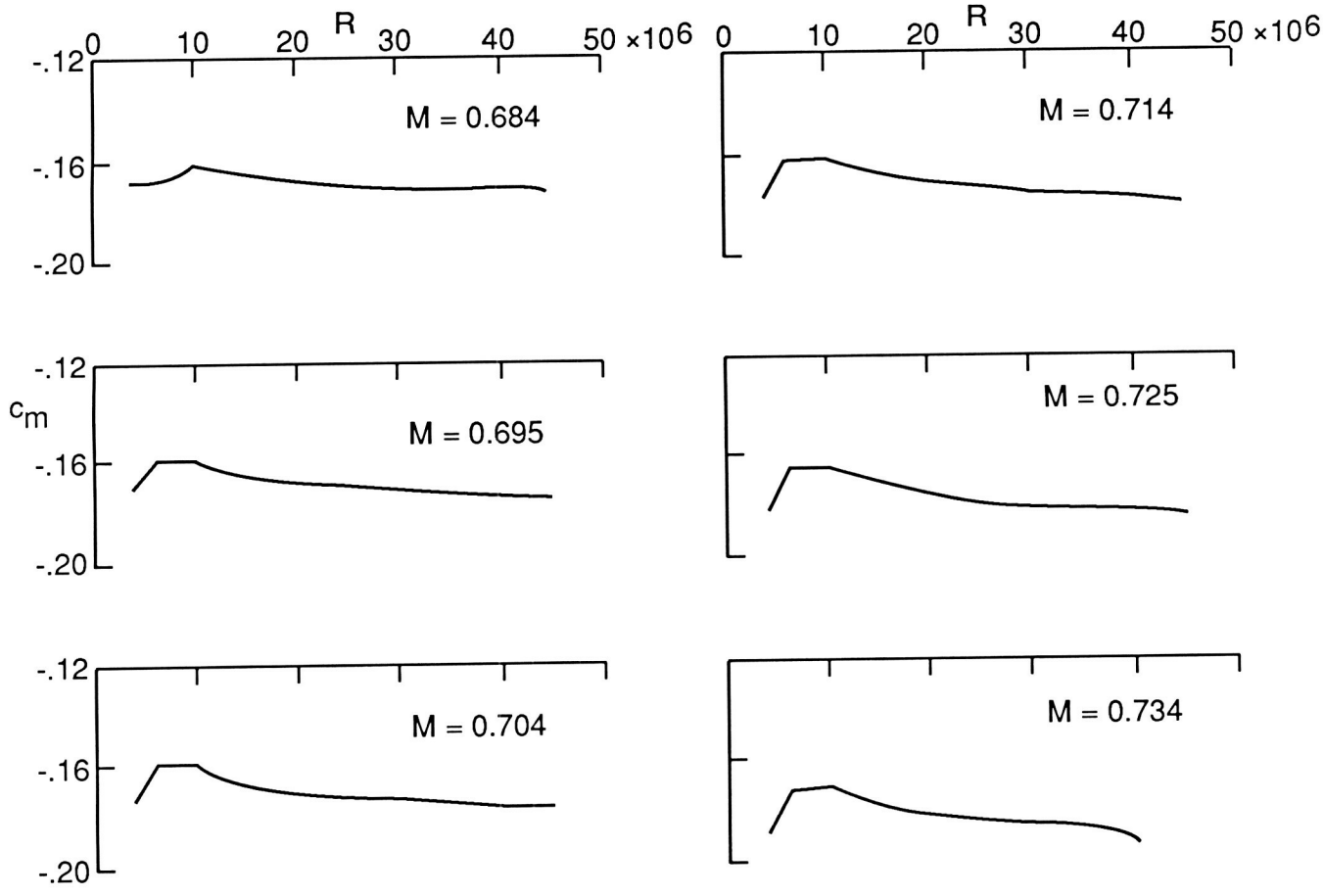

(e) $c_n = 0.71$.

Figure 11. Continued.

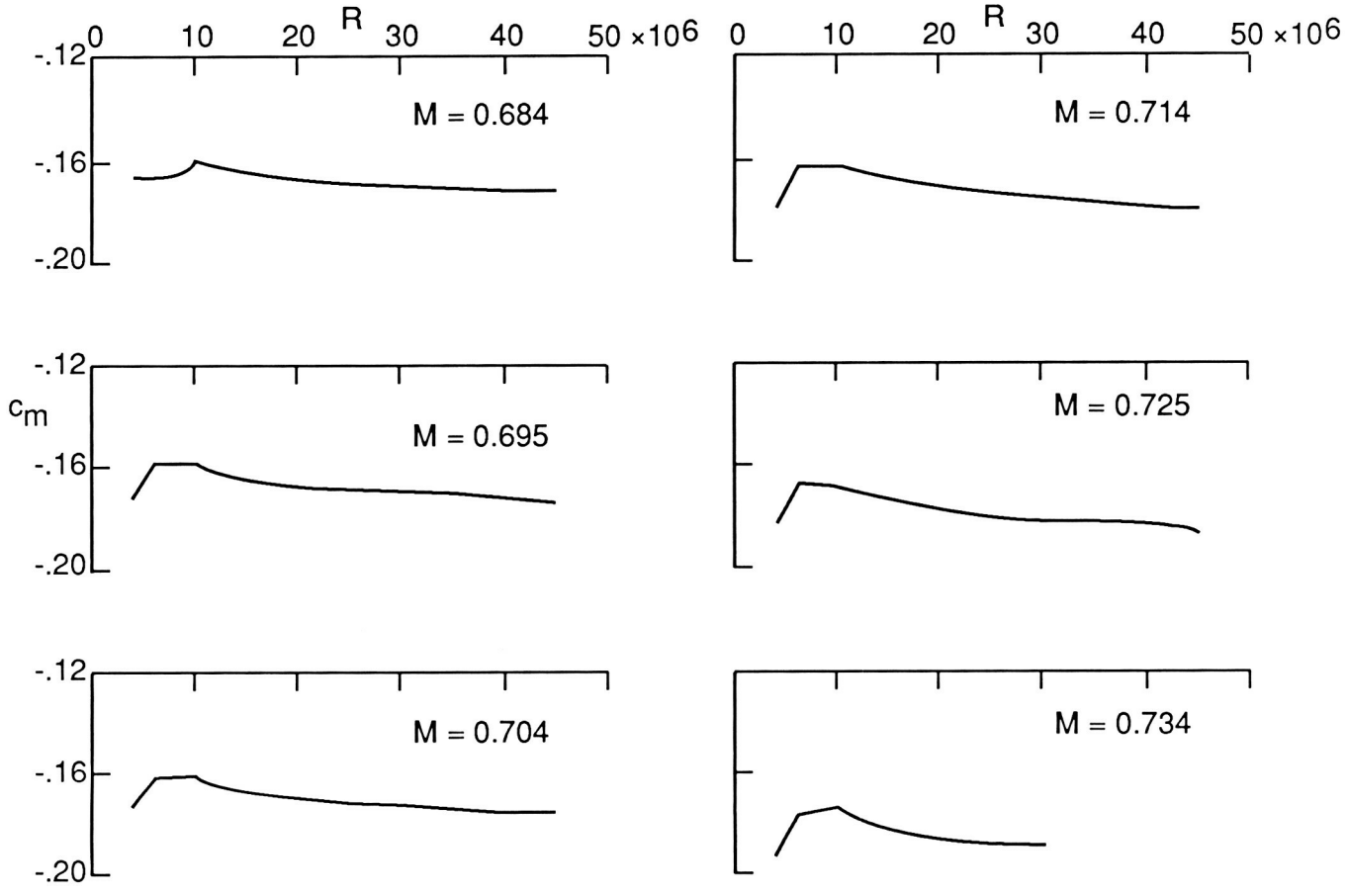

(f) $c_n = 0.76$.

Figure 11. Continued.

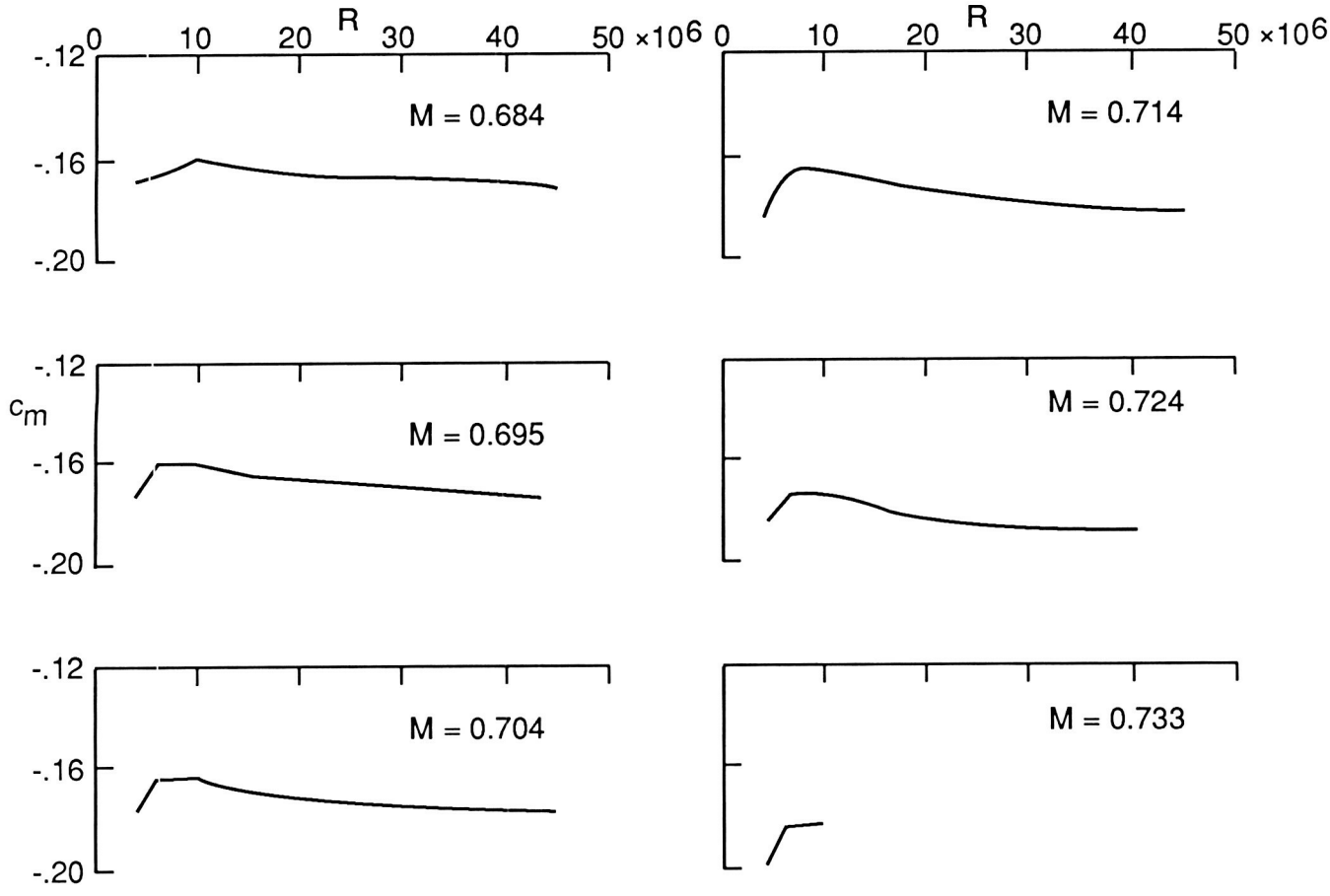

(g) $c_n = 0.81$.

Figure 11. Concluded.

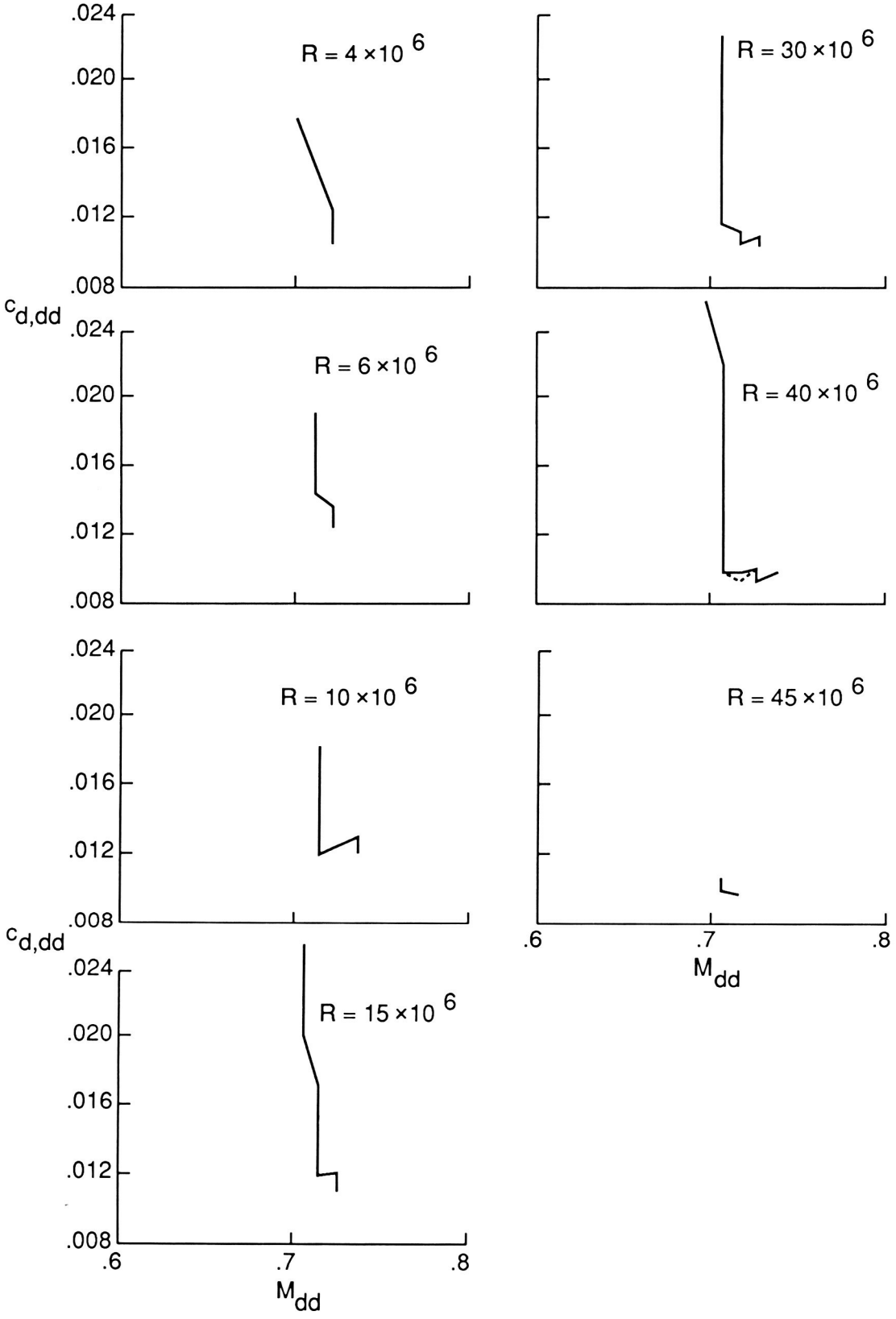

Figure 12. Drag-divergence profile-drag coefficient versus drag-divergence Mach number for seven test Reynolds numbers. Data corrected using the tables of reference 14.

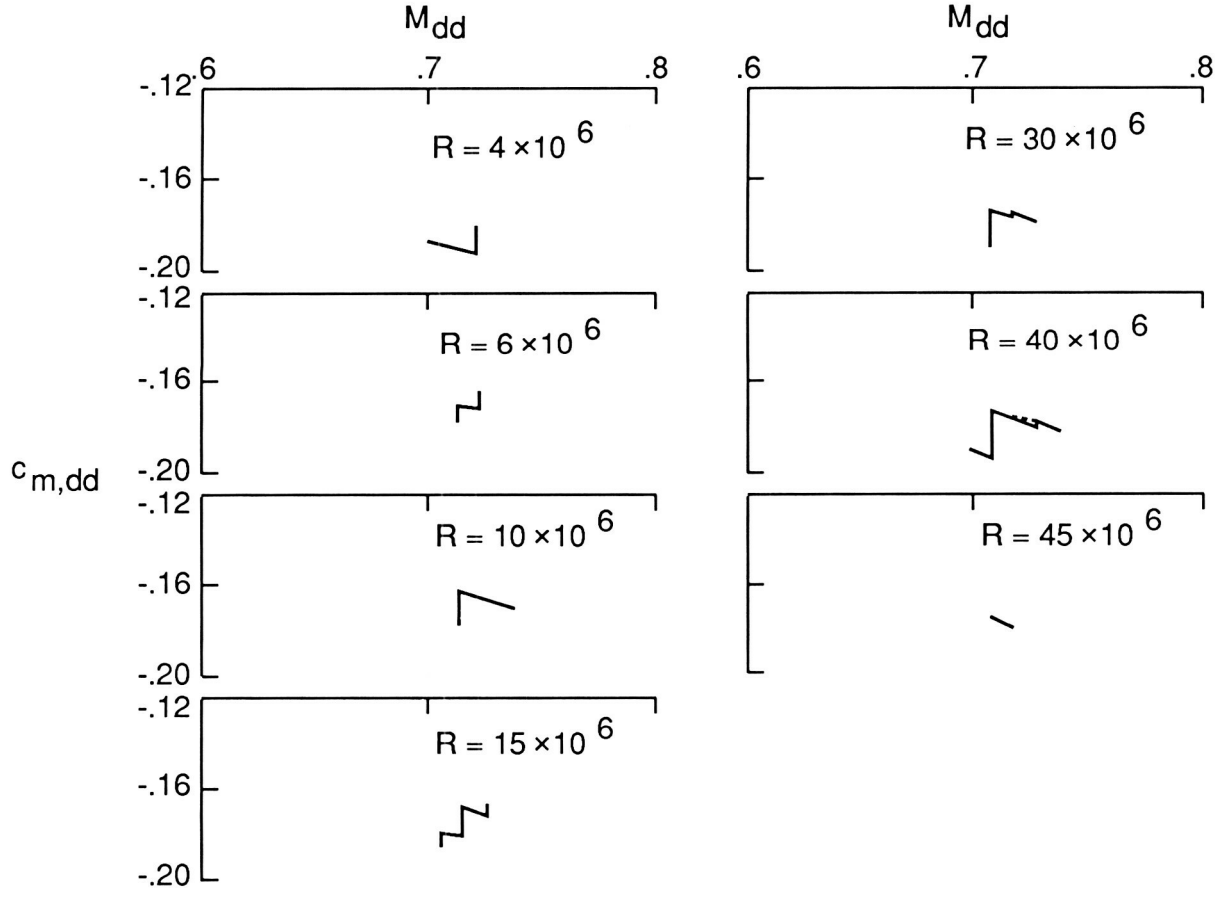

Figure 13. Drag-divergence quarter-chord pitching-moment coefficient versus drag-divergence Mach number for seven test Reynolds numbers. Data corrected using the tables of reference 14.

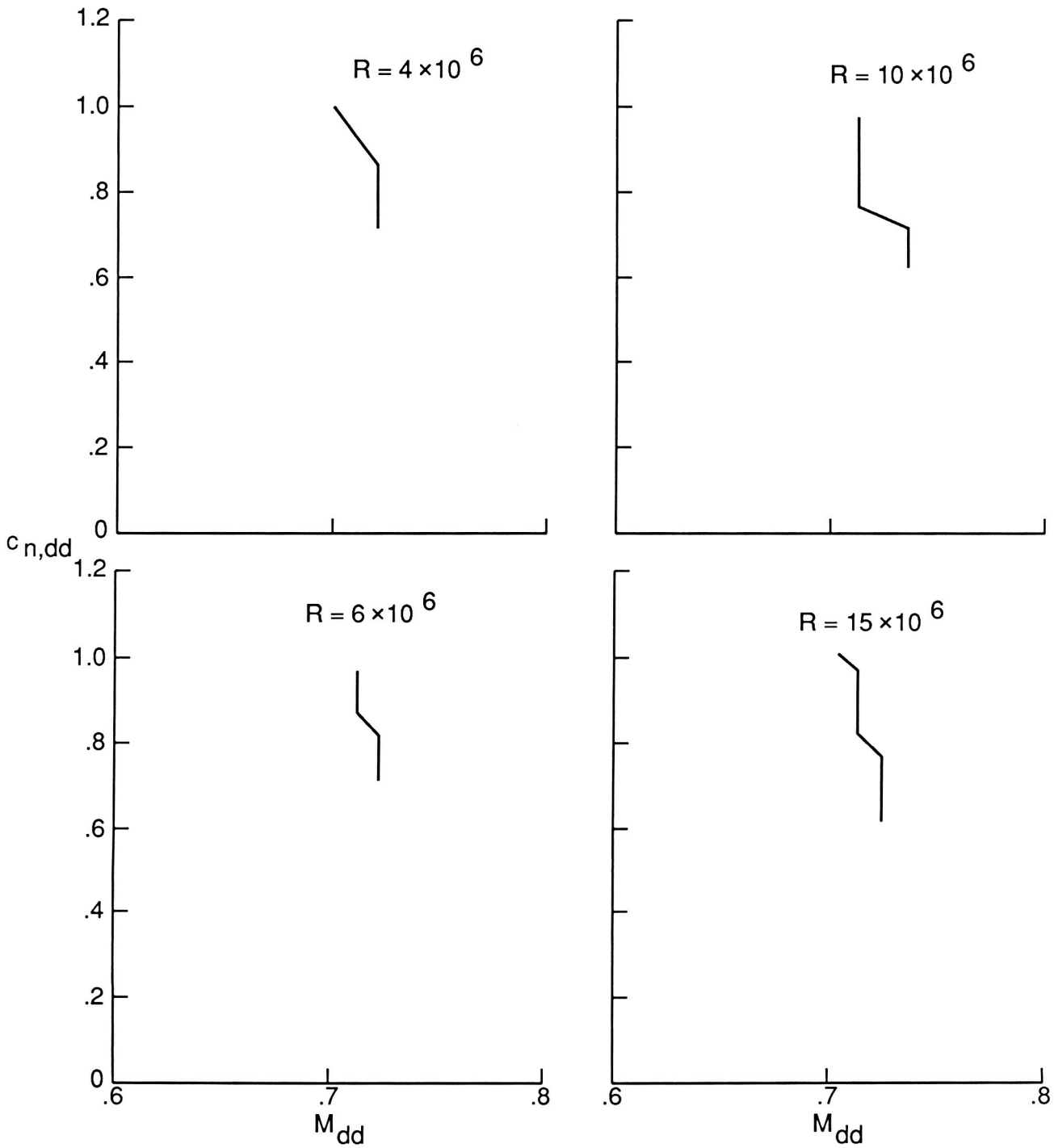

Figure 14. Drag-divergence normal-force coefficient versus drag-divergence Mach number for seven test Reynolds numbers. Data corrected using the tables of reference 14.

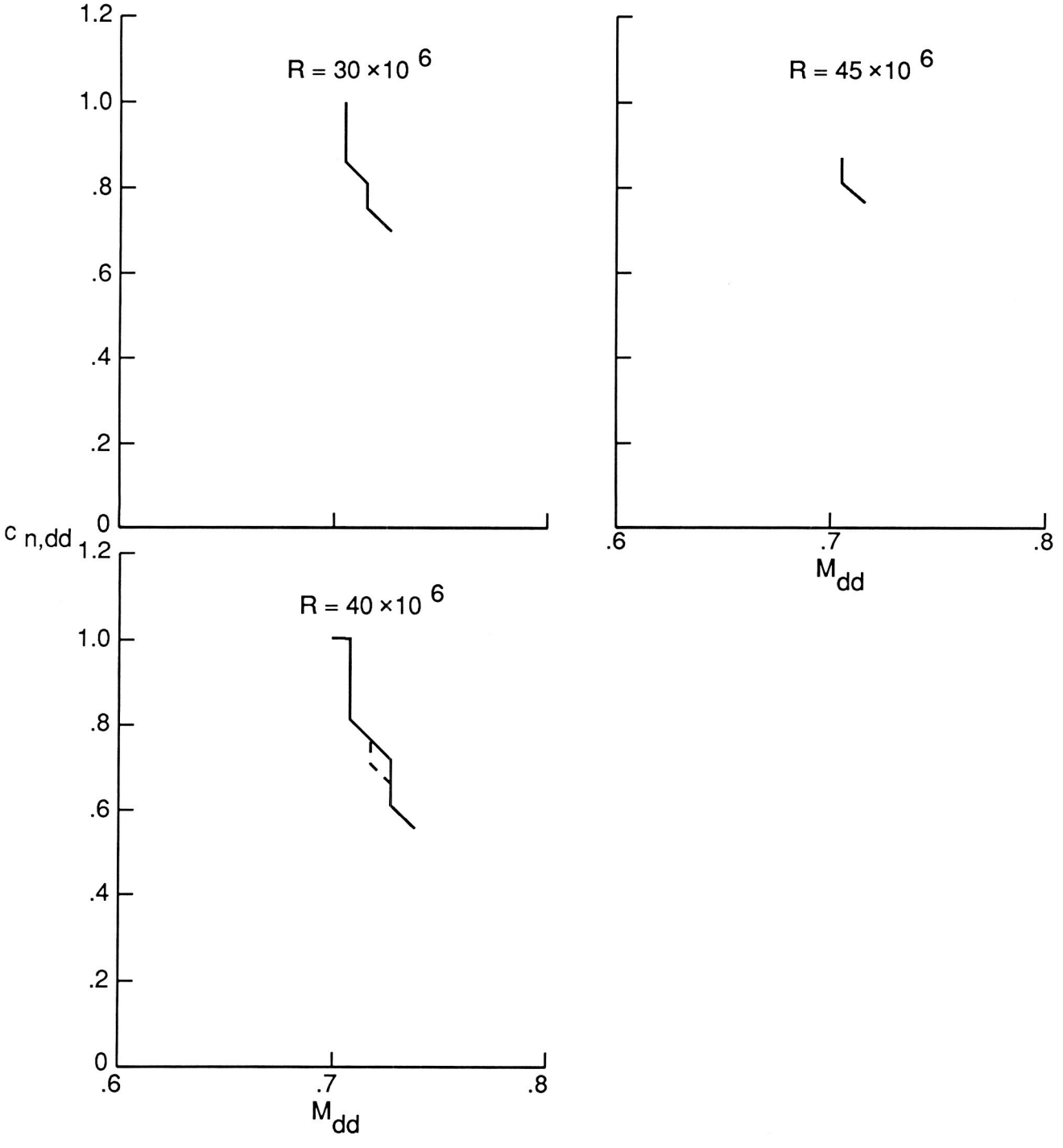

Figure 14. Concluded.

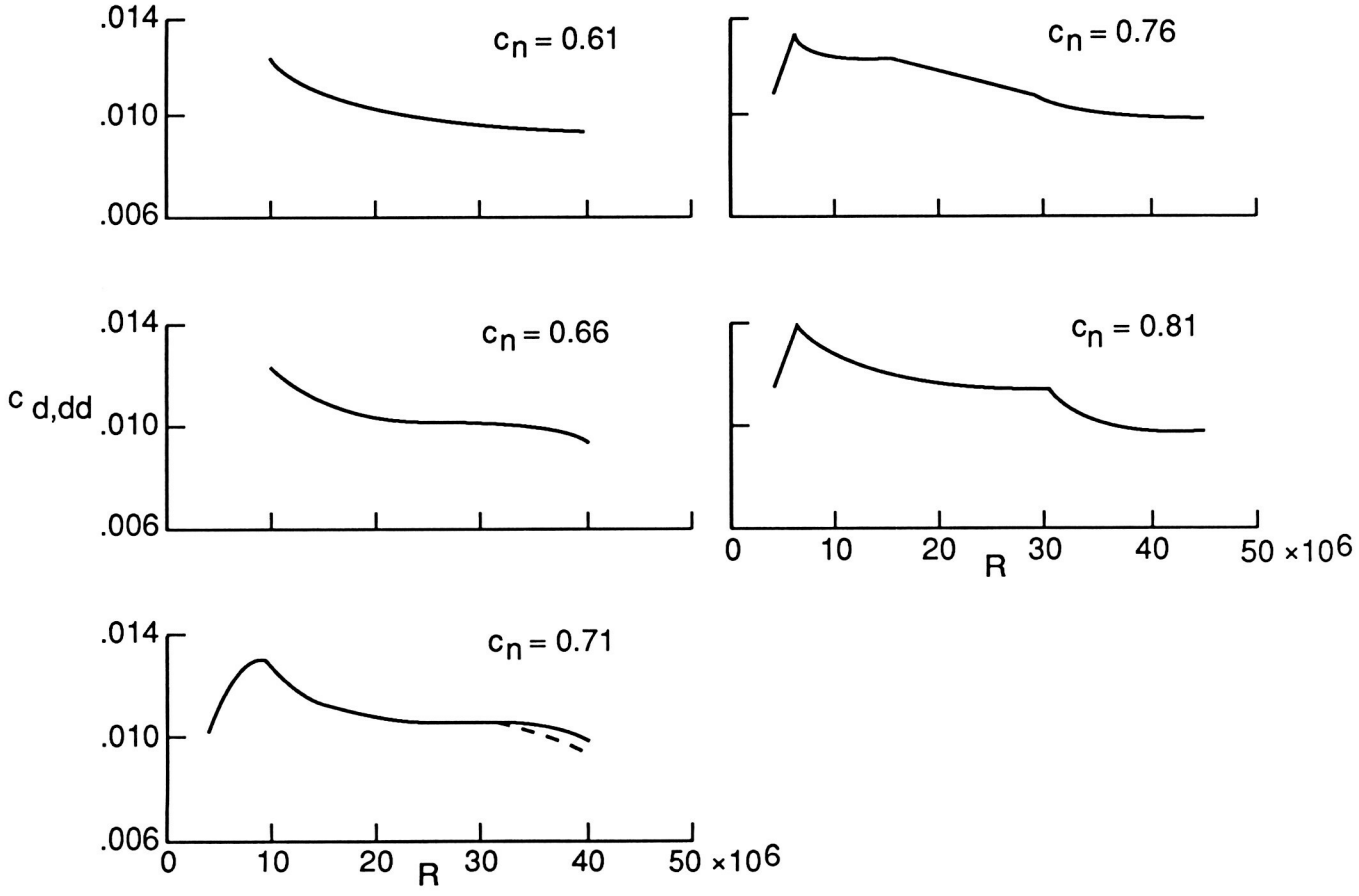

Figure 15. Drag-divergence profile-drag coefficient versus test Reynolds number for normal-force coefficients. Data corrected using the tables of reference 14.

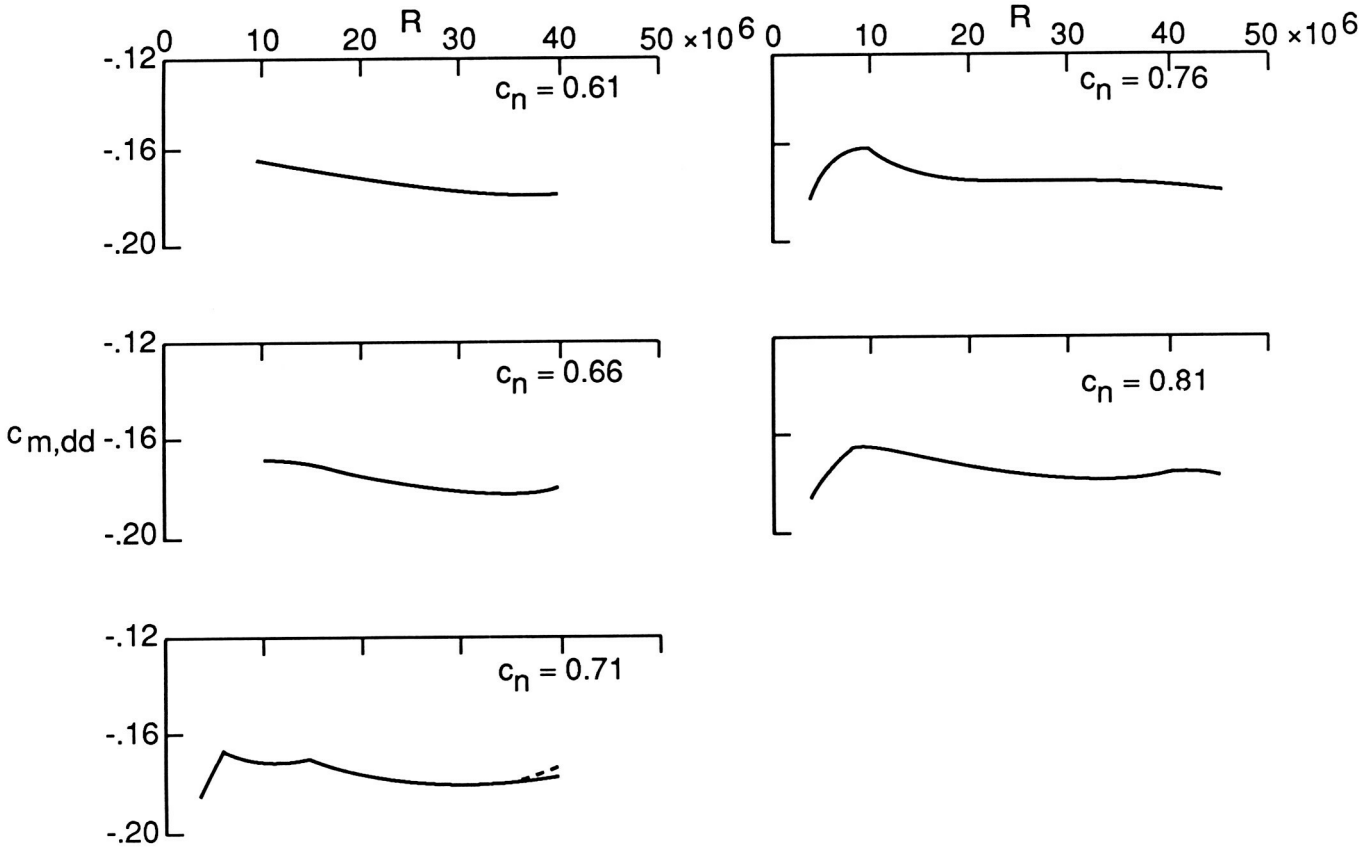

Figure 16. Drag-divergence quarter-chord pitching-moment coefficient versus test Reynolds number for normal-force coefficients. Data corrected using the tables of reference 14.

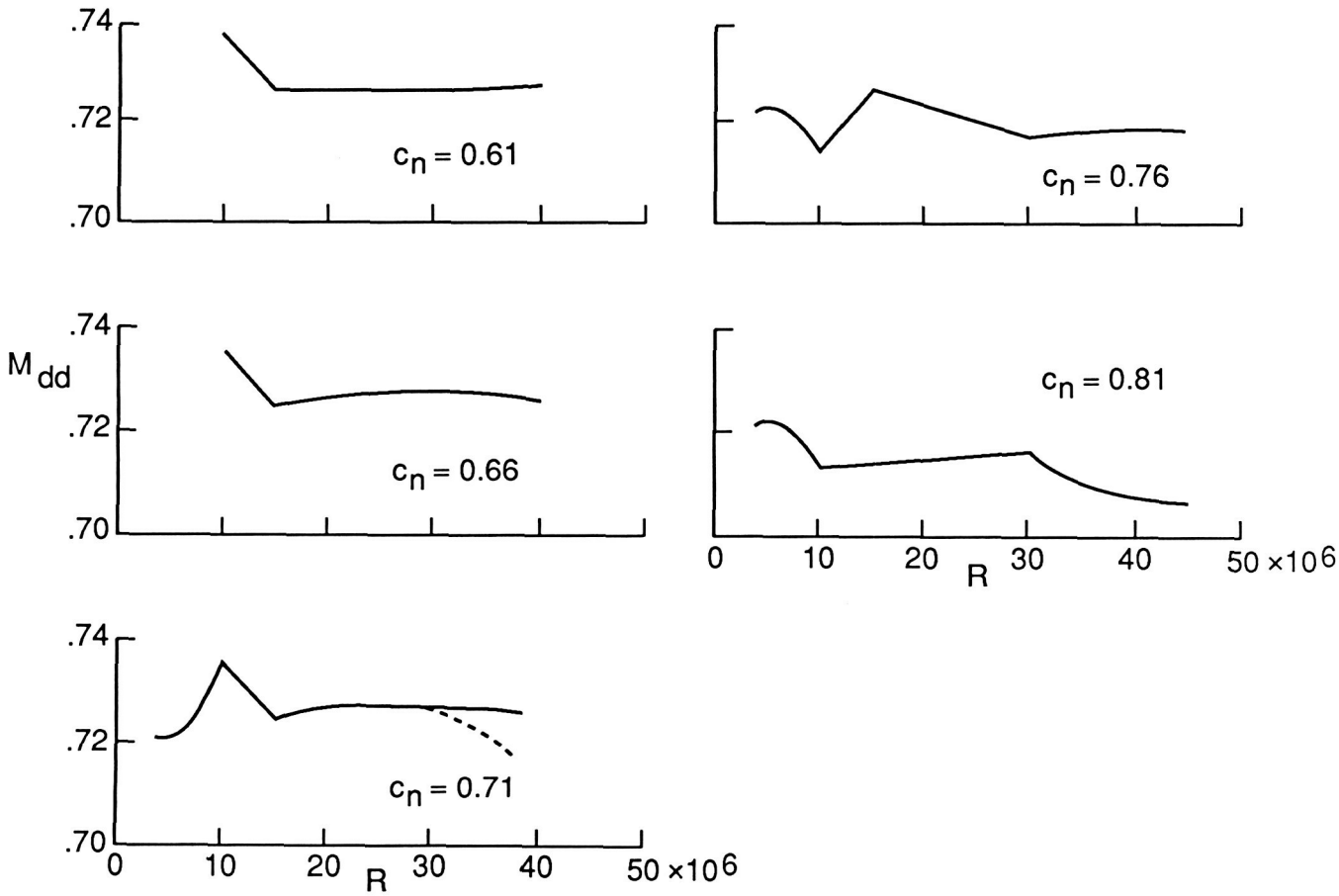

Figure 17. Drag-divergence Mach number versus test Reynolds number for normal-force coefficients. Data corrected using the tables of reference 14.

NASA
National Aeronautics and Space Administration

Report Documentation Page

1. Report No.	2. Government Accession No.	3. Recipient's Catalog No.
NASA TP-2890		

4. Title and Subtitle	5. Report Date
NASA SC(2)-0714 Airfoil Data Corrected for Sidewall Boundary-Layer Effects in the Langley 0.3-Meter Transonic Cryogenic Tunnel	March 1989
	6. Performing Organization Code
7. Author(s)	8. Performing Organization Report No.
Renaldo V. Jenkins	L-16385
9. Performing Organization Name and Address	10. Work Unit No.
NASA Langley Research Center Hampton, VA 23665-5225	505-61-01-02
	11. Contract or Grant No.
12. Sponsoring Agency Name and Address	13. Type of Report and Period Covered
National Aeronautics and Space Administration Washington, DC 20546-0001	Technical Paper
	14. Sponsoring Agency Code

15. Supplementary Notes

16. Abstract

This report presents the corrected aerodynamic data for a NASA SC(2)-0714 airfoil tested in the Langley 0.3-Meter Transonic Cryogenic Tunnel. This test was another in the series of tests involved in the joint NASA/U.S. industry Advanced Technology Airfoil Tests program. This 14-percent-thick supercritical airfoil was tested at Mach numbers from 0.6 to 0.76 and angles of attack from $-2.0°$ to $6.0°$. The test Reynolds numbers were 4×10^6, 6×10^6, 10×10^6, 15×10^6, 30×10^6, 40×10^6, and 45×10^6. Corrections for the effects of the sidewall boundary layer have been made. The uncorrected data were previously published in NASA Technical Memorandum 4044.

17. Key Words (Suggested by Authors(s))

NASA SC(2)-0714 supercritical airfoil
Cryogenic wind tunnel
Flight Reynolds number
Corrected for sidewalls

18. Distribution Statement

Unclassified—Unlimited

Subject Category 02

19. Security Classif. (of this report)	20. Security Classif. (of this page)	21. No. of Pages	22. Price
Unclassified	Unclassified	56	A04

NASA FORM 1626 OCT 86

NASA-Langley, 1989

For sale by the National Technical Information Service, Springfield, Virginia 22161-2171